AEM Accepted Manuscript Posted Online 31 May 2019
Appl. Environ. Microbiol. doi:10.1128/AEM.00560-19
Copyright © 2019 American Society for Microbiology. All Rights Reserved.

Accepted Manuscript Posted Online
Applied and Environmental Microbiology
AEM
Applied and Environmental Microbiology

# Predominance of anaerobic, spore-forming bacteria in metabolically active microbial communities from ancient Siberian permafrost

Renxing Liang[1*], Maggie Lau[1#], Tatiana Vishnivetskaya[2,3], Karen G. Lloyd[2], Wei Wang[4], Jessica Wiggins[4], Jennifer Miller[4], Susan Pfiffner[2], Elizaveta M. Rivkina[3], Tullis Onstott[1]

[1]Princeton University, Princeton, NJ, USA

[2]University of Tennessee, Knoxville, TN, USA

[3]Institute of Physicochemical and Biological Problems in Soil Science, Russian Academy of Sciences, Pushchino, Moscow Region, Russia

[4]Genomics Core Facility, Princeton University, Princeton, NJ, USA

**Running title:** Active spore-formers in ancient permafrost

[*]For correspondence

**E-mail:** rliang@princeton.edu

# Current affiliation

Laboratory of Extraterrestrial Ocean Systems, Institute of Deep-Sea Science and Engineering, Chinese Academy of Sciences, Sanya, 572000, Hainan, China

Accepted Manuscript Posted Online


## ABSTRACT

The prevalence of microbial life in permafrost up to several million years old has been well documented. However, the long-term survivability, evolution and metabolic activity of the entombed microbes over this timespan remain underexplored. We integrated aspartic acid (Asp) racemization assays with metagenomic sequencing to characterize the microbial activity, phylogenetic diversity and metabolic functions of indigenous microbial communities across a ~ 0.01 to 1.1 Ma chronosequence of continuously frozen permafrost from northeastern Siberia. Although Asp in the older bulk sediments (0.8-1.1 Ma) underwent severe racemization relative to the youngest (~0.01 Ma), the much lower D/L Asp (0.05-0.14) in the separated cells from all samples suggested that indigenous microbial communities were viable and metabolically active in ancient permafrost up to 1.1 Ma. The microbial community in the youngest sediment was the most diverse and primarily dominated by the phyla Actinobacteria and Proteobacteria. By contrast, the microbial diversity dramatically decreased in the older sediments, and anaerobic, spore-forming bacteria within Firmicutes became overwhelmingly dominant. In addition to the enrichment of sporulation-related genes, functional genes involved in anaerobic metabolic pathways such as fermentation, sulfate reduction and methanogenesis were more abundant in the older sediments. Collectively, the predominance of spore-forming bacteria and associated anaerobic metabolisms in the older sediments suggest that a subset of the original indigenous microbial community entrapped in the permafrost survived burial over geological time.




Applied and Environmental Microbiology
AEM
Applied and Environmental Microbiology

Accepted Manuscript Posted Online

Applied and Environmental Microbiology

AEM

Applied and Environmental Microbiology

47 **IMPORTANCE**

48 Understanding the long-term survivability and associated metabolic traits of microorganisms in
49 ancient permafrost frozen millions years ago provide a unique window into the burial and
50 preservation processes experienced in general by subsurface microorganisms in sedimentary
51 deposits because of permafrost's hydrological isolation and exceptional DNA preservation. We
52 employed aspartic acid racemization modeling and metagenomics to determine which microbial
53 communities were metabolically active in the 1.1 Ma permafrost from northeastern Siberia. The
54 simultaneous sequencing of extracellular and intracellular genomic DNA provided insight into
55 the metabolic potential distinguishing extinct from extant microorganisms under frozen
56 conditions over this time interval. The in-depth metagenomic sequencing advances our
57 understanding of the microbial diversity and metabolic functions of extant microbiomes from
58 early Pleistocene permafrost. Therefore, these findings extend our knowledge on the
59 survivability of microbes in permafrost from 33 Kyr to 1.1 Ma.

60

61 **Keywords:** Aspartic acid racemization, spore-forming bacteria, ancient permafrost, microbial
62 activity

63

64

65

66

67

68

69

70

Accepted Manuscript Posted Online

Applied and Environmental Microbiology

AEM

Applied and Environmental Microbiology

## INTRODUCTION

The widely distributed permafrost in the northern hemisphere represents an extreme subsurface environment of perpetual subzero temperatures with a limited influx of nutrients sustaining minimal metabolisms in the presence of *in situ* radiation from the decay of U, Th and K (1, 2). However, the persistence of DNA and a wide diversity and abundance of microbial life have been documented in permafrost deposits in Siberia, Canada and Alaska (1-3). Previous studies typically targeted total genomic DNA (3-5) that includes intracellular DNA (iDNA) from structurally intact cells (live or dead), and extracellular DNA (eDNA) released through cell lysis or actively excreted from living microbes. Although the ubiquity of eDNA is well acknowledged in many habitats, such as soil and marine sediment (6, 7), the persistence and proportion of eDNA in ancient frozen permafrost remains unknown. Furthermore, recent studies have revealed that the abundant eDNA obscures estimates of microbial diversity in soil (8) and marine sediment (9). Such concerns about relic DNA from necromass might be more prominent in ancient permafrost because eDNA will be better preserved at subzero temperatures (10). In this regard, it is important to sequence the iDNA and eDNA fractions in order to determine whether the phylogenetic diversity and function of these two DNA fractions are distinct and, if so, whether they record extant versus extinct microbial communities in ancient permafrost.

The mechanisms for long-term survival strategies by cold-adapted microorganisms in ancient permafrost have been investigated in several studies (3, 11-14). Given the harsh conditions in ancient permafrost, microbial dormancy is considered to be a major mechanism to maintain long-term viability over geological time (15). Many spore-forming bacteria within the classes *Clostridia* and *Bacilli* have been frequently cultivated from ancient permafrost in Siberia (16-19), Canada (20) and northern Norway (21). Moreover, a recent metagenomic study revealed that the relative abundance of spore-forming bacteria increased from 13% to 79% along a 19 to 33 kyr

Accepted Manuscript Posted Online

Applied and Environmental Microbiology

AEM

chronosequence in Alaskan permafrost (3). In older permafrost sediment of 400-600 kyr, two studies have found that non-spore-forming Actinobacteria were more dominant than the spore-forming Firmicutes (10, 13). These observations that spore-forming bacteria are more dominant than non-spore forming Actinobacteria in 5 to 33 kyr permafrost, but that Actinobacteria are more dominant than spore-forming bacteria in much older permafrost might reasonably be justified because spores are not metabolically active (22). Therefore, metabolic activity and DNA repair of non-spore-forming bacteria may be essential for survival in permafrost greater than 50 to 200 kyr (13, 23, 24). Although non-spore-forming bacteria such as Actinobacteria were more frequently isolated from Siberian permafrost sediments ranging in age from 10 kyr to 3 myr, the cultivation of spore-formers capable of growth at sub-zero temperatures has been reported from 3 myr old permafrost (16-19). It has been previously hypothesized that the spore-formers in ancient permafrost might be present as active vegetative cells instead of being in a dormant state (14).

Aspartic acid (Asp) racemization measurements and modeling has been utilized to constrain the microbial anabolic activity, thereby constraining the relative amounts of active versus dormant cells in marine sediments, deep subsurface fracture water and permafrost sediments (25-30). The Asp racemization model has been shown to work well in subsurface permafrost sediments with known stable temperature records and established geological ages (25, 31). According to the D/L Asp ratio of bulk sediment, the above studies (25, 31) concluded that the microbes should be metabolically active in ancient permafrost up to 25 kyr old. However, the D/L Asp values measured from the bulk sediments of greater ages (25-40 kyr) were too high to claim that the microbial activity level was higher than that required for protein maintenance (31). Since the active vegetative cells might only contribute to a small fraction of the total Asp in the



Applied and Environmental Microbiology

Accepted Manuscript Posted Online

Applied and Environmental Microbiology

AEM

frozen sediments, the D/L Asp value in cells detached from sediments would provide a more accurate estimate of the microbial activity in ancient frozen permafrost (31).

The geological ages of the permafrost sediments in the Kolyma-Indigirka Lowland of Siberia span a long chronosequence from the Holocene to the Pliocene era over a depth of 600-800 meters (32, 33). The layers of permafrost sediments harbor various types of organisms that were buried thousands to millions of years ago (31, 34). In this study, frozen sediments ranging in age from 0.01 to 1.1 Ma were selected to provide a unique window into the selective survivability and microbial activity of soil microbial communities progressively buried and isolated in permafrost through geological time under the assumption that the soil microbial communities originally present in the 1.1 Ma active layer before burial and freezing are very similar to those present in the 10 kyr active before burial and freezing (10). The phylogenetic diversity and metabolic potential of the indigenous microbial communities were interrogated with 16S rRNA amplicon and shotgun metagenomic sequencing of the eDNA and iDNA pools. Additionally, to shed light on the metabolic status and mechanisms for long-term microbial survival of the in situ microflora we measured the D/L Asp ratios in the bulk sediment samples and the separated cells. Our results suggest that the 10 kyr to 1.1 Ma permafrost chronosequence records selection of a microbial community dominated by anaerobic, spore-forming bacteria within Firmicutes that have remained metabolically active during freezing, burial and isolation over geological time from a more diverse active layer microbial community dominated by Actinobacteria and Proteobacteria that have mostly died off.



Applied and Environmental Microbiology

Accepted Manuscript Posted Online

Applied and Environmental Microbiology

AEM

## MATERIALS AND METHODS

**Sample collection for ancient permafrost sediment.** The sampling site was located within Kolyma–Indigirka Lowland in northeastern Siberia (Fig. S1). A borehole AL1-15 (69º20.44'N, 154º59.71'E; elevation of 13 m) was drilled on the floodplain close to the Alazeya River (Fig. S1) in August, 2015. The drilling operations and the aseptic techniques employed to prevent contamination have previously been described (17, 35). Permafrost cores were extracted using drilling equipment that operates without drilling fluids. This drilling method prevents down-hole contamination and reduces the environmental impact. Extracted cores were processed inside a field laboratory tent. The surfaces of 20 to 30 cm long cores were cleaned by removing melted layers with an ethyl alcohol-sterilized knife and the frozen internal parts of the cores were placed into sterile Whirl-Pak® bags and kept frozen at -15°C in powered cooler Dometic CFX 50W during storage in field and transportation. The downhole *in situ* temperature was measured immediately after coring had been completed. Permafrost sediments were collected from various intervals of the core for geochemical characterization. Three samples (1.4, 11.8 and 24.8 m below the surface) of permafrost sediments were selected for geochemical, aspartic acid and DNA analyses (Fig. 1) and transported to Princeton University on dry ice and stored at -80°C until analyses.

Permafrost can form syngenetically, where freezing occurs during sediment deposition and burial, or epigenetically, where freezing occurs long after deposition (33). The youngest permafrost sampled at 1.4 m depth was silty loam of the Yedoma suite, which was syngenetically frozen ~0.04 Ma ago. However, the age of permafrost at 1.4 m is ~0.01 Ma, late Pleistocene to early Holocene, younger than the Yedoma deposits, because the frozen sediment was thawed and refrozen in this location as indicated by absence of the large ice wedges (36).



Applied and Environmental Microbiology

Accepted Manuscript Posted Online

Applied and Environmental Microbiology

AEM

Applied and Environmental Microbiology

164 According to the stratification record (17, 37), the sediments at 11.8 m and 24.8 m were from
165 the formations of Olyor (0.8-1.6 Ma) and Tumus-Yar suites (1.8-2.2 Ma), respectively. Since the
166 permafrost at these depths was formed epigenetically, the permafrost ages at 11.8 m and 24.8 m
167 were estimated to be ~0.8-0.89 Ma and ~1-1.1 Ma (early Pleistocene), respectively.

168 **Porewater chemistry**. Anion samples were derived from pore water extracts of the internal
169 cores and concentrations fluoride, chloride, bromide, nitrite, nitrate, sulfate, phosphate, formate,
170 acetate, and proprionate were measured by an ion chromatograph coupled to an ESI-quadrupole
171 mass spectrometer (Dionex IC25 and Thermo Scientific MSQ, USA).

172 **DNA extraction and 16S rRNA amplicon sequencing**. To simultaneously extract eDNA
173 and iDNA from permafrost sediments, a procedure suitable for large-scale extraction was
174 modified from a previous study (38). Since the biomass in the ancient permafrost is typically low
175 (2), large quantities of materials (10-40 g) were used to extract iDNA and eDNA using DNeasy
176 PowerMax soil kit (Qiagen, Carlsbad, CA). Phosphate buffer (0.12 M $Na_2HPO_4$; pH 8) was
177 filter-sterilized through a 0.2-μm-pore-size membrane before being used for eDNA extraction.
178 Each 10 g permafrost sediment sample was thawed and mixed with 8.1 mL of phosphate buffer.
179 After shaking at 300 rpm for 15 min, the slurry was centrifuged at 10,000× g for 10 min at 4°C.
180 The supernatant was transferred to a new 50 mL Falcon tube without disturbing the sediment,
181 and another 8.1 mL of phosphate buffer was added to the remaining sediment. The same
182 procedure to mix the slurry was repeated and the supernatant was removed after centrifugation.
183 The combined supernatant (~16.2 mL) containing eDNA was extracted following the
184 manufacturer's procedures in the extraction kit except that the steps for bead-beating and cell
185 lysis were by-passed. The remaining sediment after eDNA removal was used to extract iDNA
186 according to the standard protocol of the same extraction kit. Sediment-free blank controls for

Accepted Manuscript Posted Online

Applied and Environmental Microbiology

AEM

eDNA and iDNA were subjected to the respective procedures as described above in order to track potential contamination introduced from the reagents and laboratory environment during extraction. The concentration of DNA was quantified using a Qubit 3.0 Fluorometer with the dsDNA HS Assay Kit (Invitrogen, Carlsbad, CA, USA). Since the DNA yield from 24.8 m was below the Qubit detection limit (0.01 ng/μL), a total of four 10 g samples were used for extraction, and the final DNA products were combined for subsequent analyses.

To prepare the library for 16S rRNA amplicon sequencing, a dual-indexed PCR amplification strategy was used to amplify the 16S rRNA gene V4 region using a universal primer set targeting most bacteria and archaea (515F/806R) (39). PCR reactions were prepared in a 25-μL (final volume) reaction mixture containing KAPA HiFi HotStart ReadyMix (12.5 μL), primers (2.5 μM, final concentration) and 1-5 μL DNA template depending on the DNA concentration. The PCR reactions consisted of initial denaturation at 94°C for 3 min; 25 or 30 cycles of denaturation at 94°C for 45 s, annealing at 50°C for 1 min, extension at 72°C for 10 min, and then a final extension step at 72°C for 10 min. The DNA extractions from sediment-free blank controls were also amplified. All amplicon products were pooled at equal molar ratio, and sequenced on Illumina Hiseq 2500 (150-bp, paired-end) in the Genomics Core Facility at Princeton University. The duel-indexed samples were demultiplexed and the raw reads were quality-filtered (Phred≥30) using Galaxy pipelines at Princeton University (http://galaxy.princeton.edu). The trimmed sequences were further analyzed by QIIME (Quantitative Insights Into Microbial Ecology) (40) using the Silva database release 128 (41). Chimeric sequences were removed and operational taxonomic units (OTUs) were clustered using a 97% similarity threshold. The alpha-diversity metrics (Chao 1 and Shannon indices) were calculated and visualized using the web-based tool MicrobiomeAnalyst (42). Statistical



Applied and Environmental Microbiology

Accepted Manuscript Posted Online

Applied and Environmental Microbiology

AEM

differences of alpha-diversity between groups of samples were computed using one-way ANOVA test in MicrobiomeAnalyst. Beta-diversity was computed using weighted and unweighted UniFrac distances and then principal coordinate analyses (PCoA) were performed to visualize the relationship and clustering among samples. Permutational multivariate analysis of variance (Adonis function in QIIME) was used to assess correlations between community composition and metadata such as geological age, depth and physiochemical properties. Venn diagrams were drawn using MetaCoMET (43) to visualize the shared and unique OTUs between iDNA and eDNA fractions.

**Shotgun metagenomic sequencing and bioinformatics analyses**. The library for shotgun metagenomic sequencing was prepared using a transposase-based method with the Nextera DNA Library Prep Kit (Illumina). Given the extremely low DNA yield in the older sediments, the procedures for library preparation were optimized by extending the cycles of PCR to 16 in order to obtain sufficiently amplified DNA for sequencing. A total of five metagenomes (1.4iDNA, 1.4eDNA, 11.8iDNA, 11.8eDNA and 24.8iDNA), ~150 million short reads (150 bp, pair end) in total, were generated on Illumina Hiseq 2500. The metagenomic sequencing for 24.8eDNA fraction was not possible because the trace amount of DNA resulted in the failure of library preparation. The raw sequences were first quality-filtered using the pipelines in Galaxy at Princeton University (http://galaxy.princeton.edu) as described above. PhyloSift was used to infer the microbial community composition from the unassembled reads of the metagenome based on the phylogeny of a suite of single-copy marker genes in the standard PhyloSift database (44). The classification of the functional genes and the relative abundance (percentage normalized to the total reads of reads) were determined using GraftM and the packages published therein (45). In addition to the packages provided in GraftM (45), customized packages were

Accepted Manuscript Posted Online

Applied and Environmental Microbiology

AEM

Applied and Environmental Microbiology

constructed to analyze functional genes related to sporulation, $O_2$ respiration (cytochrome c oxidase), sulfate reduction, and fermentation of peptides and amino acids. All raw sequences data were deposited in NCBI SRA under the Bioproject (PRJNA505516) with the accession numbers of SRR8187969 and SRR8188252-SRR8188256.

**Cell separation and enumeration by dual-staining.** In order to separate cells from ancient permafrost sediment, we adopted a previously published protocol using multiple density gradients of Nycodenz and sodium polytungstate (46). The sediment (5 g) was thawed and homogenized with 20 mL solution of 1× phosphate-buffered saline (PBS) (pH 7.4) in 50 mL Falcon tubes. To increase the efficiency of cell detachment, 2.5 mL of detergent mix (50 mM EDTA, 100 mM sodium pyrophosphate and 5% Tween 80) was added and shaken for 60 min at 500 rpm. The homogenized slurry was loaded onto a multiple density gradient consisting sodium polytungstate (2.15 g/mL) and three layers of Nycodenz (1.42, 1.27 and 1.16 g/mL) as previously described (46). All samples were then centrifuged at 15,000× g for 60 min at 4°C. The aqueous upper layers were collected and centrifuged at 12,000× g for 10 min. The pellets were resuspended with 1.5 mL PBS solution and centrifuged again at 12,000× g for 10 min. The supernatant was discarded and the cell pellets were resuspended in 1 mL PBS solution.

The LIVE/DEAD® BacLight Bacterial Viability kit (Invitrogen, Carlsbad, CA) was used to enumerate the potential live and dead cells. The live cells with intact cell membranes would be stained as green by the membrane-permeable dye (Syto9) whereas the red dye (propidium iodide, PI) can only penetrate into the membrane-compromised dead cells. Briefly, 50 µL cell suspension was mixed with 50 µL dye mixture to achieve a final concentration of Syto9 at 6 µM and PI at 30 µM. The samples were incubated in the dark for 15 min and then filtered onto a 0.2-µm black polycarbonate membrane via a vacuum system. The live (green-fluorescing) and

Accepted Manuscript Posted Online

Applied and Environmental Microbiology

AEM

Applied and Environmental Microbiology

potentially dead (red-fluorescing) cells were visualized and imaged using Epifluorescence microscopy (Olympus BX60, Olympus America Inc., Melville, NY).

**Asp racemization assay by high performance liquid chromatography (HPLC)**. The sediment (1 g) was mixed with 1.5 N HCl (1 mL) to remove carbonate as previously described (25). The demineralized sediment was dried and then hydrolyzed by adding 10 mL 6 N HCl as described in a previous study (26). The hydrolysis was performed at 105ºC for 16 h under $N_2$ and then the reactions were stopped on ice to cool down. An aliquot of the hydrolysate (100 µL) was transferred into glass vials and dried under fume hood. The dried residues were dissolved in 1 mL Milli-Q water and dried again on a speed vacuum concentrator. The final hydrolyzed products were dissolved in 4 mL Milli-Q water and stored at -20ºC prior to analysis. To hydrolyze the separated cells, the cell suspension (0.5 mL) was centrifuged at 14,000× g for 5 min and then 6N HCl (0.5 mL) was added to resuspend the pellet. The homogenized cell suspension was incubated 105ºC for 16 h under $N_2$ as described above. The hydrolysate (100 µL) was dried and then dissolved in 1mL Milli-Q water. To reduce interference in Asp detection, 5-10 µL NaOH (1N) was added to each sample and immediately centrifuged at 14,000× g for 5 min to remove any soluble iron after precipitation. The supernatant was filtered (0.2 µm) and stored at -20°C prior to HPLC analysis.

To quantify D- and L-Asp acids in hydrolysate, a modified HPLC procedure was adopted from a previous study (26). The amino acids were derivatized with o-phthaldialdehyde/N-acetyl-L-cysteine as previously described (27) and immediately analyzed by HPLC. HPLC (PU-1580, JASCO, Japan equipped with a Water C18 column (Nova Pak@ c18, 300 by 3.9mm; 5-mm particle size, Waters, USA) and a fluorescence detector (Jasco FP-1520, Japan). D- and L-Asp acids were eluted with a binary mobile phase consisting methanol and 50 mM sodium acetate

Accepted Manuscript Posted Online

buffer (pH 5.4). The flow rate was 0.6 mL/min and the gradient condition can be found in Table S1. Triplicate measurements were performed for all samples. Background racemization during hydrolysis at high temperature were determined and subtracted from the D/L Asp values measured for the samples as suggested in a previous study (27). All glassware used during hydrolysis and other steps were treated with 4N HCl and baked at 450°C overnight to remove any residual amino acid contamination. Blanks with no sediment were run in parallel and no significant D- or L-Asp was detected in blanks as compared with samples.

The racemization rate was calculated according to the Arrhenius equation:

$$k = Ae^{(\frac{E_a}{RT})} \quad (1)$$

in which $k$ is the racemization rate constant, $E_a$ is the activation energy (kJ mol$^{-1}$), $A$ is the frequency factor, $R$ refers to the universal gas constant ($8.314\times10^{-3}$ kJ K$^{-1}$ mol$^{-1}$) and $T$ is temperature in K. The kinetic parameters of Asp racemization in permafrost sediment (25) were used to extrapolate the specific racemization rate constant of each sample based on the *in situ* temperatures at corresponding depths (Table S2). We assumed the temperature of the sediment has been stable under frozen conditions and predicted the D/L Asp values for each depth using the equation 2 below:

$$ln_t\left[\frac{1+\mathrm{D/L}}{1-\mathrm{D/L}}\right] - ln_0\left[\frac{1+\mathrm{D/L}}{1-\mathrm{D/L}}\right] = 2kt \quad (2)$$

where D/L refers to the ratio of D-Asp to L-Asp and t is time.

## RESULTS AND DISCUSSION

**Geochemical characteristics**. The *in situ* temperature ranged from -2 to -6°C at 1 to 25 m depth in the borehole (Fig. 1). These temperatures were higher than the mean annual temperature of wells drilled (-11 to -13°C) in Kolyma Lowland area in 2002 (25). The pH was slightly acidic



Applied and Environmental Microbiology
AEM
Applied and Environmental Microbiology

Accepted Manuscript Posted Online

Applied and Environmental Microbiology

AEM

Applied and Environmental Microbiology

(6.22 - 6.93) in the upper layers (0.8 - 4.6 m) whereas the deeper strata exhibited more neutral pHs, varying from 7.03 to 7.88 (Fig. 1). The concentrations of methane in the core sediment varied widely from 4 to 200 µmol/kg at various intervals (Fig. 1). The detection of ancient methane and methanogenic activity has been frequently reported from Siberian permafrost in previous studies (33, 35). The major anions ($Cl^-$, $SO_4^{2-}$, $NO_2^-$ and $NO_3^-$) in the water extracts from the three depths (1.4, 11.8 and 24.8m) were generally <10 µg/g with slight variations (Table S2). As reported in a previous study (32), the presence of various electron acceptors could be utilized by indigenous microorganisms to drive denitrification and sulfate reduction in this particular site.

**Asp racemization in bulk sediment**. The concentration of L-Asp in the youngest layer (1.54±0.06 µmol/g) was approximately 22 times higher than that of the older sediments (0.07±0.01 µmol/g) (Fig. 2A). D-Asp was also detected (up to 0.37±0.03 µmol/g at 1.4m) and the concentration showed a similar decreasing trend with depth as that of L-Asp (Fig. 2A). Interestingly, the D/L Asp values in the bulk sediment increased with the geological age (Fig. 2B). The increase of D/L Asp ratios with geological age has been previously shown in Siberian permafrost up to 0.04 Ma old (25, 31) and in sub-seafloor sediment up to several million years old (26, 28, 29, 47). Therefore, our results confirmed that Asp in buried sediment were subjected to racemization through geological time even at subzero temperatures in frozen permafrost. Since temperature is a major factor influencing racemization, the racemization rate of Asp has been extrapolated to subzero temperature (-4°C) in marine sediment based on heating experiments in a previous study (48). If the initial D/L Asp in the bulk sediment before freezing is assumed to be zero, then the Asp racemization in the older sediments would achieve

Accepted Manuscript Posted Online

Applied and Environmental Microbiology

AEM

Applied and Environmental Microbiology

equilibrium with a D/L of 1 (Fig. 2B). Obviously, the actual D/L Asp was much lower than 1 (Fig. 2) thereby suggesting that the microbial cells in the deeper, older permafrost were sufficiently metabolically active to maintain a low D/L Asp, but calculation of an in situ metabolic rate would require further amino acid analyses and assumptions regarding the metabolic yields and protein repair processes of the active microorganisms (27).

**Cell separation and cellular D/L Asp**. Since D- and L-Asp in the bulk sediments originated from total biomass and necromass present in the sediment, it is critical to separate cells from sediments and determine the cellular D/L Asp in ancient permafrost. Both green- and red fluorescently stained cells of different morphologies and sizes were observed in all samples (Fig. S2). The total cell counts decreased dramatically with depth and age (Fig. S2 and S3), which is consistent with fluorescently stained cell counts of marine (26, 28) and lake (49, 50) sediments. Notably, the percentage of potentially viable cells (22.8%) at 1.4 m was similar to that in coastal marine sediment (51), and permafrost from Alaska (3) and northern Norway (21). It should be noted that membrane-compromised cells are not necessarily dead and membrane integrity does not guarantee microbial activity (51), particularly in ancient permafrost with numerous stressors.

Consistent with the observed trend in the bulk sediment (Fig. 2A), the concentration of Asp in separated cells from youngest sample (1.03±0.08 nmol/g) was much higher than that from the deeper and older sediments at 11.8 and 24.8 m (0.15±0.01 and 0.17 ±0.01 nmol/g, respectively). However, the cellular Asp content only accounted for a small fraction (~0.05-0.2%) of the total Asp in the bulk sediment. Interestingly, the D/L Asp values in the cells (0.05-0.14) were much smaller than that of the bulk sediment at each depth (Fig. 2B). This range overlaps the 0.02 and 0.12 D/L Asp values of bacterial cultures (27, 29). Furthermore, the D/L Asp values in cells extracted from sub-seafloor sediment and deep fracture fluids were 0.014-0.085 (52) and 0.037-

Accepted Manuscript Posted Online

Applied and Environmental Microbiology

AEM

Applied and Environmental Microbiology

348 0.095 (27), respectively. Therefore, the D/L Asp values from separated cells in ancient
349 permafrost were similar to those determined from live pure cultures and active microflora in
350 different subsurface environments. More importantly, the actual values of D/L Asp in separated
351 cells was much less than the predicted D/L Asp due to purely chemical racemization at all depths
352 (Fig. 2B). Together with the evidence from live cell staining (Fig. S2 and 3), we conclude that
353 the extant microbial communities are viable and are sufficiently metabolically active to maintain
354 a relatively low D/L ratio at subzero temperatures in ancient permafrost up to 1.1 Ma old.

355 **Microbial diversity**. Previous studies showed that amplifiable DNA products were only
356 detected in permafrost samples younger than 400-600 kyr due to severe DNA damage (10, 13).
357 In our study, detectable and amplifiable DNA was obtained in much older permafrost of up to
358 1.1 Ma (Table S3). The decreasing trend for total DNA yield (Table S3) with geological age was
359 consistent with previous reports in ancient permafrost samples up to 400-600 kyr (10, 13).
360 Alpha-diversity (Chao1 and Shannon indices) dramatically decreased with age (Fig. S4), which
361 is consistent with previous findings in ancient permafrost in Siberia (10, 13) and Alaska (3).
362 Principal coordinate analysis revealed that microbial communities determined from iDNA and
363 eDNA fractions were significantly different ($p<0.001$) from one another (Fig. S5).
364 Permutational multivariate analysis of variance revealed that the variation in beta-diversity
365 among iDNA fractions could be largely explained by depth (42%, $F=2.9$, $p<0.05$) and age (51%,
366 $F=4.1$, $p<0.01$). That the depth and age were found to be the primary determinants probably
367 reflects the depletion of nutrients and the long-term exposure to cold temperature and highly
368 reduced conditions in the deeper/older sediments through geological time. The eDNA analyses
369 of the 11.8 m and 24.8 m samples, however, closely clustered to that of the blank controls as
370 shown by weighed Unifrac PCoA analysis (Fig. S7B). Therefore, many OTUs in the eDNA

Accepted Manuscript Posted Online

Applied and Environmental Microbiology

AEM

fractions at 11.8 and 24.8 m originated from the common contaminants from reagents and the laboratory environment (53) and do not reflect environmental parameters.

As revealed by 16S rRNA amplicon and metagenomic sequencing of iDNA fractions (Fig. 3 and S6), the relative abundance of Actinobacteria, Acidobacteria and Chloroflexi decreased with geological age. The phylum Firmicutes was overwhelmingly predominant in the iDNA fractions from the older sediments at 11.8 and 24.8 m (Fig. 3 and S6). Despite the difference in relative abundance between 11.8 and 24.8 m, most of these microbial lineages were identified as belonging to the class Clostridia (Fig. S6 and S7) that is typically comprised of anaerobic, spore-forming bacteria. Although the majority of the OTUs (35.8-87.2%) were exclusively present in the iDNA fractions (Fig. S8), 267 OTUs are shared among all the iDNA fractions (Fig. 4). The shared community was mainly comprised of the phyla Firmicutes, Actinobacteria, Proteobacteria and Chloroflexi (Fig. S8). These microbial lineages commonly found in soil are apparently persistent in permafrost irrespective of the geological age. More interestingly, 44.5% of the total OTUs (1293) in the iDNA of the 11.8 m sample were shared with those of the 1.4 m sample, whereas the iDNA of the 11.8 and 24.8 m samples shared only 10.5% of their total number of OTUs (Fig. S8). The overlapping OTUs between the young and old permafrost sediments has been previously reported (10), suggesting that the original microflora present in the deepest older sediments share some similarity with the microbial community in the youngest, shallowest permafrost layer. These shared OTU's provide an opportunity to examine species level changes over the course of depositional time and as a function of isolation from the surface with increasing subsurface isolation time upon freezing. Recovery of draft genomes of these ancient



Applied and Environmental Microbiology

Accepted Manuscript Posted Online

Applied and Environmental Microbiology

AEM

and modern microbial species with deeper sequencing would provide further information about the mechanism and long-term evolution in cryogenic environments throughout geological time.

The eDNA fractions represent a mixture of nucleic acids excreted from the extant microbial communities and lysed microbial cells. In the youngest permafrost sediment the number of OTUs unique to the 16S rRNA gene amplicons of the eDNA fraction was 2,095 and likely represent lysed microbial cell, whereas 10,139 OTUs were shared with the iDNA fraction and might represent 16S rRNA genes of recently lysed microbial cells or an artifact from DNA extraction process (Fig. 4). In the deep, older sediments, however, most of the OTUs in the iDNA fractions were unique (~70-90%) and a much smaller proportion of the eDNA pool was unique, only 150 OTUs in the case of the 11.8 m sample. This suggests that little of the DNA from lysed cells (unique OTUs in the eDNA) survives for 1.1 Ma in a frozen state. However, caution should be exercised because the absence of OTUs in either eDNA or iDNA fraction could also be attributed to the detection limit of the approach employed in this study. The spore-forming bacteria within Firmicutes were predominant amongst the unique OTUs of the iDNA pools, whereas Actinobacteria and Proteobacteria were more abundant in unique OTUs from eDNA fractions (Fig. 4 and S9). Such differences between inferred physiology of the ancient relic DNA (unique OTUs in the eDNA) versus that of the iDNA suggest that most aerobes became extinct whereas the spore-forming bacteria affiliated within the phylum Firmicutes survived the ~1 million years of entrapment in the ancient permafrost.

By comparison the percentage of overlapping OTUs between iDNA and eDNA fractions in the coastal soil of the Atacama Desert of Chile was 88% and that of the hyperarid core soils of the Atacama Desert were 20% (54). Since a portion of the 16S rRNA gene of the eDNA pool can be continually replenished by turnover of microbial biomass (55), Schulze-Makuch et al. (54)



Applied and Environmental Microbiology

Accepted Manuscript Posted Online

Applied and Environmental Microbiology

AEM

Applied and Environmental Microbiology

argued that the microbial activity in coastal soil was much higher than that of the hyper arid core due to the greater humidity and nutrient abundance. The overlap in OTUs from our results ranged from 53% for the youngest permafrost to 6-25% for the oldest permafrost (Fig. 4 and S9) and suggests that like the Atacama Desert the microbial activity in the youngest permafrost sediment was likely much higher than the older permafrost sediments due to the higher temperature (Fig. 1) and availability of labile organic matter in the Yedoma deposit (56).

**Predominance of anaerobic metabolisms in the deeper sediments.** The subsequent functional analyses of the five metagenomes provided further evidence that the potential metabolic pathways of the microbial communities became predominantly anaerobic in the deeper, older strata (11.8 and 24.8 m) relative to the youngest layer which were enriched with genes related to aerobic metabolism. For example, genes encoding various types of cytochrome oxidases were only enriched (Fig. 5A) in the Holocene sediment from the Yedoma suite (Fig. 1). The relative abundance of high $O_2$ affinity terminal oxidases (microaerobic, cbb3- and bd-types) were more abundant than low-$O_2$ affinity terminal oxidases (aerobic; aa3- type), suggesting microaerobic metabolism dominates in the top Yedoma permafrost layer (Fig. 1). The genes linked to aerobic oxidation of methane (particulate methane monooxygenase gene, *pmo*A), ammonia (ammonia monooxygenase, *amoA* and hydroxylamine oxidoreductase, hao) and methanol (methanol dehydrogenase, mxaF) were only detected in the 1.4 m sample. The genes associated with the denitrification pathway (*napA*, *nirK and nosZ* genes) were enriched in the 1.4 m sample relative to the deeper samples (Fig. 5A). By contrast, the functional genes linked to anaerobic metabolism such as dissimilatory sulfate reduction (dissimilatory sulfite reductase, *DsrA* and *DsrB*), methanogenesis (α-subunit of methyl-coenzyme M reductase, *McrA*) and $H_2$ production (Fe-Fe hydrogenase) were more abundant in the deeper sediments particularly at

Accepted Manuscript Posted Online

Applied and Environmental Microbiology

AEM

Applied and Environmental Microbiology

24.8m (Fig. 5A). The potential for anaerobic metabolism deduces from the metagenomic data suggests that highly reduced, anoxic conditions were created in the deeper frozen sediment to support anaerobic microbial respiration with various electron acceptors (32). For the youngest, shallowest permafrost sediment where cell turnover appears to have been the greatest the metagenomic data suggest either that a microaerophilic environment was captured at the time of freezing or that diffusion of $O_2$ from the overlying active layer through patchy epigenetic pore ice is sustaining microaerophilic respiration today.

**Long-term survival strategies in Pleistocene permafrost**. A suite of sporulation-related genes were found highly enriched in the metagenomes of the deeper samples compared to their relative abundance in the metagenome of youngest permafrost sediment (Fig. 5B), which is not surprising given the predominance of anaerobic, spore-forming bacteria (mostly *Clostridia*) in the deeper, older layers (Fig. 3). Among them, Spo0A, *spoIIGA* and *spoIVB* are involved in various stages of sporulation (57, 58). The *dpaA* and *spoVA* genes are involved in synthesis and transport of dipicolinic acid (DPA) (59), whereas SASPs genes encode for small, acid soluble proteins (SASPs) in spores (60). The high level of DPA in spores and complexation of DNA by SASPs are important for the long-term survival of spores (61). Notably, the gene for encoding spore photoproduct lyase (*SplA*), which is known for DNA repair caused by UV radiation (62), was also enriched in the deeper samples. Additionally, other genes (*recA* and *ykoV*) that are potentially important in DNA repair (63, 64) were detected with high abundance from all samples (Fig. 5B). Intriguingly, the gene encoding the protein repair enzyme (Protein L-Isoaspartyl / D-Aspartyl O-Methyltransferase, PIMT) was present in low abundance at all depths (Fig. 5B). Therefore, the PIMT is a plausible means through which the low cellular D/L Asp (Fig. 2B) was maintained by converting isomerized (iso-Asp) or racemized (D-Asp) back to L-Asp

Accepted Manuscript Posted Online

Applied and Environmental Microbiology

AEM

Applied and Environmental Microbiology

462 residues in metabolically active microbial cells (65). Since PIMT is only found in Gram-negative
463 bacteria and archaea (66), the dominant Gram-positive spore-forming bacteria from the older
464 permafrost are either replacing their enzymes deactivated by Asp racemization or they repairing
465 their damaged proteins by an unknown mechanism. Both require metabolic activity, but less for
466 the latter than the former.

467 The overwhelmingly predominant spore-forming bacteria (Fig. 4) and enrichment of
468 sporulation-related genes (Fig. 5B) in the iDNA fraction of older sediments (0.8-1.1 Ma)
469 indicates microbial dormancy might play a critical role in long-term survival under frozen
470 conditions. The increase of spore-forming bacteria in older permafrost was broadly similar to a
471 recent study of Alaskan permafrost up to 33 kyr in age (3), but contradicts other studies from
472 Siberia permafrost up to 400-600 kyr (10, 13). The greater abundance of non-spore forming
473 bacteria (Actinobacteria) over spore formers (Firmicutes) in these older permafrost samples were
474 ascribed to the metabolic activity and DNA repair of non-spore-forming bacteria (13, 24). Due
475 to the lack of high energy compounds in dormant endospores (67), microorganisms buried in
476 ancient permafrost must maintain low levels of metabolic activity to repair DNA and protein
477 damage in order to survive through geological time. Therefore, the predominant spore-forming
478 bacteria in the older permafrost of this study should be in an active metabolic state instead of
479 dormancy (14). Such postulation was corroborated by several lines of evidence including the low
480 D/L cellular Asp (Fig. 2B), live cell staining (Fig. S3 and S5) and predominance of spore-
481 forming bacteria in iDNA pools from the older permafrost (Fig. 4 and S6-7). Due to limited
482 nutrient influx in the sealed, frozen systems, it's possible that the dominant spore-forming
483 bacteria survived as persisters that can maintain minimum activity to repair DNA and proteins
484 over prolonged periods of time (14).

Accepted Manuscript Posted Online

Applied and Environmental Microbiology

AEM

**Microbial interactions involved in the metabolism of ancient carbon**. The ancient permafrost represents a large reservoir of organic carbon that can be utilized by the indigenous microbial community (2, 37). Not surprisingly, genes involved in the degradation of different carbon compounds were detected at all depths with varying abundance (Fig. 6A. The relative abundance of genes for hydrolysis of labile sugars such as starch (amylase) and sucrose (sucrase) was much higher in the youngest sediment (Fig. 6A). In contrast, the genes responsible for degradation of recalcitrant carbon (xylosidase and galactosidase) were more abundant in the deeper, older sediments (Fig. 6A). The enrichment of genes involved in utilizing various carbohydrates has also been reported in 19-33 kyr old Alaskan permafrost (3). Apart from fermentation of carbohydrates, numerous proteolytic enzymes from the family cysteine (C) peptidases, metallo (M) peptidases and serine (S) peptidases (68) were detected in all three permafrost samples (Fig. 6B). However, those peptidases (clostripai, papain and pyroglutamyl peptidase) from anaerobic protein-degrading microorganisms (69) were more numerically abundant in the older strata. Furthermore, the key genes involved in intracellular biodegradation of amino acids were highly enriched in the deeper, older sediment as compared with the youngest layer (Fig. 6B). For instance, the ferredoxin-reducing oxidoreductases specific for aldehydes, 2-ketoisovalerate ferredoxin oxidoreductases and indolepyruvate ferredoxin oxidoreductase were more abundant (Fig. 6B). These ferredoxin-reducing oxidoreductases are highly $O_2$-sensitive (70) and were known to be involved in the breakdown of both non-aromatic and aromatic amino acids in *Clostridium* species (71). Therefore, the dominant bacteria associated with *Clostridia* in the deep, ancient permafrost have the genetic potential to cycle detrital proteins and further ferment amino acids throughout the geological time.



Applied and Environmental Microbiology

Accepted Manuscript Posted Online

Applied and Environmental Microbiology

AEM

Due to the potential of fermentative capabilities by the predominant spore-forming *Clostridia*, genes involved in the production of formate (pyruvate formate lyase), acetate (acetate kinase) and butyrate (butanol dehydrogenase and butyrate kinase) were more numerically abundant in the older sediments (Fig. 6B). These fatty acids generated from fermentative processes can be utilized by sulfate-reducing bacteria and syntrophic bacteria detected in the older permfrost sediments. For example, the most dominant sulfate-reducing bacteria, *Desulfosporosinus*, are able to oxidize short-chain fatty acids (e.g., acetate, propionate and butyrate) with sulfate, nitrate and Fe(III) as electron acceptors (72, 73). Additionally, several syntrophic bacteria from the genera *Syntrophomonas* and *Smithella* were detected in the older permafrost. These microbial lineages are well-known for their capability of syntrophically oxidizing fatty acids when coupled with hydrogenotrophic methanogens (74, 75). Notably, small fractions (less than 1%) of hydrogenotrophic methanogens (mainly *Methanoregula*) were detected in the iDNA fraction from the older strata. The *mcrA* sequences from the older sediments showed the highest similarity to *Methanoregula formicica* SMSP$^{T}$, an isolate from methanogenic sludge (76), and *Methanoregula boonei* 6A8, isolated from acidic peat bog (77). Furthermore, the relative abundance of key enzyme acetyl-CoA synthase involved in autotrophic $CO_2$ fixation (Wood-Ljungdahl pathway) were highly enriched in the older permafrost relative to the youngest permafrost. The presence of acetyl-CoA synthase and its role in anabolic $CO_2$ fixation have been reported in the genome of *Methanoregula formicica* SMSP$^{T}$ (76) and *Methanoregula boonei* 6A8 (77). Since various amounts of $CH_4$ were indeed detected at different depths of the borehole (Fig. 1) with $\delta^{13}C$ values of -85‰ VPDB (78), the identified archaeal lineages from the genus *Methanoregula* in the older sediments might contribute to methane production by utilizing $CO_2$ and $H_2$ in the sealed, frozen ecosystem with limited nutrient flux.



Applied and Environmental Microbiology

Accepted Manuscript Posted Online

Applied and Environmental Microbiology

AEM

Applied and Environmental Microbiology

## Conclusions

The ubiquity of relic DNA in many habitats including water, soil and sediment has raised some concerns on its impact on microbial community diversity estimates (8, 9, 79). We simultaneously extracted the DNA from intact cells, iDNA, and the extracellular DNA, eDNA, potentially representing past, relic microbial lineages preserved in a 0.01-1.1 Ma chronosequence of permanently frozen sediments along. The OTUs in the eDNA that are not shared with those of the iDNA pools suggested that certain ancient species became extinct (i.e., not members of metabolically active subsurface permafrost communities) whereas other microorganisms represented by OTUs in the iDNA pool remained active through geological time. The overlapping core community among iDNA pools from all samples (Fig. S8) indicated that a subset of microorganisms in the older layers was also present in the youngest permafrost in Yedoma deposit. The predominance of anaerobic, spore-forming bacteria in the iDNA fractions from the older permafrost suggested that microbial dormancy might have played important roles in maintaining long-term survivability over the prolonged periods of geological time. Due to the lack of metabolic activity in dormant spores, the predominant spore-forming bacteria might be present as active, vegetative cells instead of dormant forms in order to maintain the observed low cellular D/L Asp. Indeed, the live cell-staining and Asp racemization assay of the separated cells indicated that many indigenous microorganisms buried in the oldest permafrost in Northern Hemisphere might represent living microbial communities that are metabolically active. Due to the low DNA yield and limited sequencing depth, no metagenome-assembled genomes (MAGs) could be recovered to further elucidate the adaption and evolution mechanisms of the survived

Accepted Manuscript Posted Online

553 microbial populations in the ancient permafrost. With a combination of metagenomics and
554 single-cell amplified genomes (SAGs), a previous study has revealed that the evolutionary
555 changes of microbial genomes were undetectable in subsurface marine sediments of thousands
556 years old (80). Therefore, future studies should be pursued to recover MAGs or SAGs to
557 confirm whether the survived species have undergone adaptive evolution in frozen sediments
558 that are millions of years old.

559 **Acknowledgement**

560 This research was supported by an NSF DEB-1442059 and NSF EAR-1528492 to TCO, NSF
561 DEB-1442262 and International Research Experience for Students grant IIA-1460058 to TV, and
562 by Russian Government Assignment AAAA-A18-118013190181-6,PP ARCTICA AAAA-A18-
563 118013190182-3 to ER.

564

565 **Conflict of interest**

566 The authors declare that they have no conflicts of interest.

567 **References**

568 1. Steven, B., R . Leveille, W.H. Pollard, and L.G. Whyte. 2006. Microbial ecology and
569 biodiversity in permafrost. Extremophiles **10**:259-267.
570 2. Jansson JK, Taş N. 2014. The microbial ecology of permafrost. Nat Rev Microbiol
571 12:414.
572 3. Mackelprang R, Burkert A, Haw M, Mahendrarajah T, Conaway CH, Douglas TA,
573 Waldrop MP. 2017. Microbial survival strategies in ancient permafrost: insights from
574 metagenomics. The ISME journal 11:2305.



Applied and Environmental Microbiology
AEM
Applied and Environmental Microbiology

Accepted Manuscript Posted Online


4. Lau MC, Stackhouse B, Layton AC, Chauhan A, Vishnivetskaya T, Chourey K, Ronholm J, Mykytczuk N, Bennett P, Lamarche-Gagnon G. 2015. An active atmospheric methane sink in high Arctic mineral cryosols. The ISME journal 9:1880.

5. Chauhan A, Layton AC, Vishnivetskaya TA, Williams D, Pfiffner SM, Rekepalli B, Stackhouse B, Lau MC, Phelps TJ, Mykytczuk N. 2014. Metagenomes from thawing low-soil-organic-carbon mineral cryosols and permafrost of the Canadian high Arctic. Genome Announc 2:e01217-14.

6. Torti A, Lever MA, Jørgensen BB. 2015. Origin, dynamics, and implications of extracellular DNA pools in marine sediments. Mar genomics 24:185-196.

7. Nagler M, Insam H, Pietramellara G, Ascher-Jenull J. 2018. Extracellular DNA in natural environments: features, relevance and applications. Appl Microbiol Biotechnol:1-14.

8. Carini P, Marsden PJ, Leff JW, Morgan EE, Strickland MS, Fierer N. 2017. Relic DNA is abundant in soil and obscures estimates of soil microbial diversity. Nat Microbiol 2:16242.

9. Torti A, Jørgensen BB, Lever MA. 2018. Preservation of microbial DNA in marine sediments: Insights from extracellular DNA pools. Environ Microbiol 20: 4526-4542.

10. Willerslev E, Hansen AJ, Rønn R, Brand TB, Barnes I, Wiuf C, Gilichinsky D, Mitchell D, Cooper A. 2004. Long-term persistence of bacterial DNA. Curr Biol 14:R9-R10.

11. Vorobyova E, Soina V, Mulukin A. 1996. Microorganisms and enzyme activity in permafrost after removal of long-term cold stress. Adv Space Res 18:103-108.

12. Mulyukin AL, Soina VS, Demkina EV, Kozlova AN, Suzina NE, Dmitriev VV, Duda VI, El GI. Formation of resting cells by non-spore-forming microorganisms as a strategy of




Applied and Environmental Microbiology
AEM
Applied and Environmental Microbiology

Accepted Manuscript Posted Online

long-term survival in the environment, p 208-219. *In* (ed), International Society for Optics and Photonics, 2003.

13. Johnson SS, Hebsgaard MB, Christensen TR, Mastepanov M, Nielsen R, Munch K, Brand T, Gilbert MTP, Zuber MT, Bunce M. 2007. Ancient bacteria show evidence of DNA repair. Proc Natl Acad Sci 104:14401-14405.

14. Lewis K, Epstein S, Godoy VG, Hong S-H. 2008. Intact DNA in ancient permafrost. Trends Microbiol 16:92-94.

15. Kryazhevskikh N, Demkina E, Manucharova N, Soina V, Gal'chenko V. 2012. Reactivation of dormant and nonculturable bacterial forms from paleosoils and subsoil permafrost. Microbiology 81:435-445.

16. Bakermans C, Tsapin AI, Souza-Egipsy V, Gilichinsky DA, Nealson KH. 2003. Reproduction and metabolism at -10°C of bacteria isolated from Siberian permafrost. Environ Microbiol 5:321-326.

17. Shi T, Reeves R, Gilichinsky D, Friedmann E. 1997. Characterization of viable bacteria from Siberian permafrost by 16S rDNA sequencing. Microb Ecol 33:169-179.

18. Vishnivetskaya TA, Petrova MA, Urbance J, Ponder M, Moyer CL, Gilichinsky DA, Tiedje JM. 2006. Bacterial community in ancient Siberian permafrost as characterized by culture and culture-independent methods. Astrobiology 6:400-414.

19. Vatsurina A, Badrutdinova D, Schumann P, Spring S, Vainshtein M. 2008. *Desulfosporosinus hippei* sp. nov., a mesophilic sulfate-reducing bacterium isolated from permafrost. Int J Syst Evol Microbiol 58:1228-1232.

20. Steven B, Briggs G, McKay CP, Pollard WH, Greer CW, Whyte LG. 2007. Characterization of the microbial diversity in a permafrost sample from the Canadian



Applied and Environmental Microbiology
AEM
Applied and Environmental Microbiology

Accepted Manuscript Posted Online

high Arctic using culture-dependent and culture-independent methods. FEMS Microbiol Ecol 59:513-523.

21. Hansen AA, Herbert RA, Mikkelsen K, Jensen LL, Kristoffersen T, Tiedje JM, Lomstein BA, Finster KW. 2007. Viability, diversity and composition of the bacterial community in a high Arctic permafrost soil from Spitsbergen, Northern Norway. Environ Microbiol 9:2870-2884.

22. Setlow P. 1994. Mechanisms which contribute to the long-term survival of spores of Bacillus species. Appl Microbiol 76: 49S-6OS.

23. Amato P, Doyle SM, Battista JR, Christner BC. 2010. Implications of subzero metabolic activity on long-term microbial survival in terrestrial and extraterrestrial permafrost. Astrobiology 10:789-798.

24. Dieser M, Battista JR, Christner BC. 2013. Double-strand DNA break repair at -15°C. Appl Environ Microbiol. 79:7662–7668.

25. Brinton KL, Tsapin AI, Gilichinsky D, McDonald GD. 2002. Aspartic acid racemization and age-depth relationships for organic carbon in Siberian permafrost. Astrobiology 2:77-82.

26. Langerhuus AT, Røy H, Lever MA, Morono Y, Inagaki F, Jørgensen BB, Lomstein BA. 2012. Endospore abundance and D:L-amino acid modeling of bacterial turnover in holocene marine sediment (Aarhus Bay). Geochim Cosmochim Acta 99:87-99.

27. Onstott TC, Magnabosco C, Aubrey A, Burton A, Dworkin J, Elsila J, Grunsfeld S, Cao B, Hein J, Glavin D. 2014. Does aspartic acid racemization constrain the depth limit of the subsurface biosphere? Geobiology 12:1-19.



Applied and Environmental Microbiology
AEM
Applied and Environmental Microbiology

Accepted Manuscript Posted Online

642 28. Braun S, Mhatre SS, Jaussi M, Røy H, Kjeldsen KU, Pearce C, Seidenkrantz M-S,
643 Jørgensen BB, Lomstein BA. 2017. Microbial turnover times in the deep seabed studied
644 by amino acid racemization modelling. Sci Rep 7:5680.
645 29. Lomstein BA, Langerhuus AT, D'Hondt S, Jørgensen BB, Spivack AJ. 2012. Endospore
646 abundance, microbial growth and necromass turnover in deep sub-seafloor sediment.
647 Nature 484:101.
648 30. Møller MH, Glombitza C, Lever MA, Deng L, Morono Y, Inagaki F, Doll M, Su C-c,
649 Lomstein BA. 2018. D: L-amino acid modeling reveals fast microbial turnover of days to
650 months in the subsurface hydrothermal sediment of Guaymas Basin. . Front Microbiol
651 9:967.
652 31. Tsapin AI, McDonald G. Permafrost: Proceedings of the Eighth International Conference
653 on Permafrost, 21-25 July 2003, Zurich, Switzerland, p 1141-1144. *In* Phillips M,
654 Springman SM, Arenson LU (ed), Balkema,
655 32. Rivkina E, Gilichinsky D, Wagener S, Tiedje J, McGrath J. 1998. Biogeochemical
656 activity of anaerobic microorganisms from buried permafrost sediments. Geomicrobiol J
657 15:187-193.
658 33. Rivkina E, Shcherbakova V, Laurinavichius K, Petrovskaya L, Krivushin K, Kraev G,
659 Pecheritsina S, Gilichinsky D. 2007. Biogeochemistry of methane and methanogenic
660 archaea in permafrost. FEMS Microbiol Ecol 61:1-15.
661 34. Rivkina E, Laurinavichius K, McGrath J, Tiedje J, Shcherbakova V, Gilichinsky D. 2004
662 Microbial life in permafrost. Adv Space Res33:1215-1221.
663 35. Rivkina E, Petrovskaya L, Vishnivetskaya T, Krivushin K, Shmakova L, Tutukina M,
664 Meyers A, Kondrashov F. 2016. Metagenomic analyses of the late Pleistocene



Applied and Environmental Microbiology
AEM
Applied and Environmental Microbiology

Accepted Manuscript Posted Online

665 permafrost–additional tools for reconstruction of environmental conditions.
666 Biogeosciences 13:2207-2219.
667 36. Rivkina E, Abramov A, Spirina E, Petrovskaya L, Shatilovich A, Shmakova L,
668 Scherbakova V, Vishnivetskaya T. 2018. Earth's perennially frozen environments as a
669 model of cryogenic planet ecosystems. Permafrost Periglacial Processes 29:246-256.
670 37. Shmelev D, Veremeeva A, Kraev G, Kholodov A, Spencer RG, Walker WS, Rivkina E.
671 2017. Estimation and sensitivity of carbon storage in permafrost of North-Eastern
672 Yakutia. Permafr Periglac Process 28:379-390.
673 38. Taberlet P, Prud'homme S.M., Campione E, Roy J, Miquel C, Shehzad W, Gielly L,
674 Rioux D, Choler P, Clément J.C. 2012. Soil sampling and isolation of extracellular DNA
675 from large amount of starting material suitable for metabarcoding studies. Mol Ecol
676 21:1816-1820.
677 39. Caporaso JG, Lauber CL, Walters WA, Berg-Lyons D, Huntley J, Fierer N, Owens SM,
678 Betley J, Fraser L, Bauer M. 2012. Ultra-high-throughput microbial community analysis
679 on the Illumina HiSeq and MiSeq platforms. ISME J. 6:1621.
680 40. Caporaso JG, Kuczynski J, Stombaugh J, Bittinger K, Bushman FD, Costello EK, Fierer
681 N, Pena AG, Goodrich JK, Gordon JI. 2010. QIIME allows analysis of high-throughput
682 community sequencing data. Nature Methods 7:335.
683 41. Quast C, Pruesse E, Yilmaz P, Gerken J, Schweer T, Yarza P, Peplies J, Glöckner FO.
684 2012. The SILVA ribosomal RNA gene database project: improved data processing and
685 web-based tools. Nucleic Acids Res 41:D590-D596.



Applied and Environmental Microbiology
AEM
Applied and Environmental Microbiology

Accepted Manuscript Posted Online


42. Dhariwal A, Chong J, Habib S, King IL, Agellon LB, Xia J. 2017. MicrobiomeAnalyst: a web-based tool for comprehensive statistical, visual and meta-analysis of microbiome data. Nucleic Acids Res 45:W180-W188.

43. Wang Y, Xu L, Gu YQ, Coleman-Derr D. 2016. MetaCoMET: a web platform for discovery and visualization of the core microbiome. Bioinformatics 32:3469-3470.

44. Darling AE, Jospin G, Lowe E, Matsen IV FA, Bik HM, Eisen JA. 2014. PhyloSift: phylogenetic analysis of genomes and metagenomes. PeerJ 2:e243.

45. Boyd JA, Woodcroft BJ, Tyson GW. 2018. GraftM: a tool for scalable, phylogenetically informed classification of genes within metagenomes. Nucleic Acids Res 46:e59-e59.

46. Morono Y, Terada T, Kallmeyer J, Inagaki F. 2013. An improved cell separation technique for marine subsurface sediments: applications for high‐throughput analysis using flow cytometry and cell sorting. Environ Microbiol 15:2841-2849.

47. Lomstein BA, Jørgensen BB, Schubert CJ, Niggemann J. 2006. Amino acid biogeo-and stereochemistry in coastal Chilean sediments. Geochim Cosmochim Acta 70:2970-2989.

48. Steen AD, Jørgensen BB, Lomstein BA. 2013. Abiotic racemization kinetics of amino acids in marine sediments. PLoS One 8:e71648.

49. Haglund A-L, Lantz P, Törnblom E, Tranvik L. 2003. Depth distribution of active bacteria and bacterial activity in lake sediment. FEMS Microbiol Ecol 46:31-38.

50. Kallmeyer J, Grewe S, Glombitza C, Kitte JA. 2015. Microbial abundance in lacustrine sediments: a case study from Lake Van, Turkey. Int J Earth Sci 104:1667-1677.

51. Luna G, Manini E, Danovaro R. 2002. Large fraction of dead and inactive bacteria in coastal marine sediments: comparison of protocols for determination and ecological significance. Appl Environ Microbiol 68:3509-3513.




Applied and Environmental Microbiology
AEM
Applied and Environmental Microbiology

Accepted Manuscript Posted Online

52. Braun S, Morono Y, Becker KW, Hinrichs K-U, Kjeldsen KU, Jørgensen BB, Lomstein BA. 2016. Cellular content of biomolecules in sub-seafloor microbial communities. Geochim Cosmochim Acta 188:330-351.

53. Salter SJ, Cox MJ, Turek EM, Calus ST, Cookson WO, Moffatt MF, Turner P, Parkhill J, Loman NJ, Walker AW. 2014. Reagent and laboratory contamination can critically impact sequence-based microbiome analyses. BMC Biology 12:87.

54. Schulze-Makuch D, Wagner D, Kounaves SP, Mangelsdorf K, Devine KG, de Vera J-P, Schmitt-Kopplin P, Grossart H-P, Parro V, Kaupenjohann M. 2018. Transitory microbial habitat in the hyperarid Atacama Desert. Proc Natl Acad Sci 115:2670-2675.

55. Levy-Booth DJ, Campbell RG, Gulden RH, Hart MM, Powell JR, Klironomos JN, Pauls KP, Swanton CJ, Trevors JT, Dunfield KE. 2007. Cycling of extracellular DNA in the soil environment. Soil Biol Biochem 39:2977-2991.

56. Vonk JE, Mann PJ, Davydov S, Davydova A, Spencer RG, Schade J, Sobczak WV, Zimov N, Zimov S, Bulygina E. 2013. High biolability of ancient permafrost carbon upon thaw. Geophys Res Lett 40:2689-2693.

57. Onyenwoke RU, Brill JA, Farahi K, Wiegel J. 2004. Sporulation genes in members of the low G+C Gram-type-positive phylogenetic branch (Firmicutes). Arch Microbiol 182:182-192.

58. Brown DP, Ganova-Raeva L, Green BD, Wilkinson SR, Young M, Youngman P. 1994. Characterization of spo0A homologues in diverse *Bacillus* and *Clostridium* species identifies a probable DNA-binding domain. Mol Microbiol 14:411-426.

59. Donnelly ML, Fimlaid KA, Shen A. 2016. Characterization of *Clostridium difficile* spores lacking either SpoVAC or DPA synthetase. J Bacteriol 198:1694-1707.



Applied and Environmental Microbiology
AEM
Applied and Environmental Microbiology

Accepted Manuscript Posted Online


60. Setlow P. 2007. I will survive: DNA protection in bacterial spores. Trends Microbiol 15:172-180.

61. Setlow P. 1994. Mechanisms which contribute to the long-term survival of spores of Bacillus species. J Appl Bacteriol 76:49S-60S.

62. Xue Y, Nicholson WL. 1996. The two major spore DNA repair pathways, nucleotide excision repair and spore photoproduct lyase, are sufficient for the resistance of *Bacillus subtilis* spores to artificial UV-C and UV-B but not to solar radiation. Appl Environ Microbiol 62:2221-2227.

63. Cox MM. 1999. Recombinational DNA repair in bacteria and the RecA protein. Progress in Nucleic Acid Research and Molecular Biology 63: 311-366.

64. Hiom K. 2003. DNA repair: bacteria join in. Curr Biol 13:R28-R30.

65. Li C, Clarke S. 1992. A protein methyltransferase specific for altered aspartyl residues is important in Escherichia coli stationary-phase survival and heat-shock resistance. Proc Natl Acad Sci 89:9885-9889.

66. Li C, Clarke S. 1992. Distribution of an L-isoaspartyl protein methyltransferase in eubacteria. J Bacteriol 174:355-361.

67. Setlow P. 2006. Spores of *Bacillus subtilis*: their resistance to and killing by radiation, heat and chemicals. . J Appl Microbiol 101:514-525.

68. Rawlings ND, Barrett AJ, Bateman A. 2009. MEROPS: the peptidase database. Nucleic Acids Res 38:D227-D233.

69. Lloyd KG, Schreiber L, Petersen DG, Kjeldsen KU, Lever MA, Steen AD, Stepanauskas R, Richter M, Kleindienst S, Lenk S. 2013. Predominant archaea in marine sediments degrade detrital proteins. Nature 496:215-218.




Applied and Environmental Microbiology
AEM
Applied and Environmental Microbiology

Accepted Manuscript Posted Online

70. Hall D, Cammack R, Rao K. 1971. Role for ferredoxins in the origin of life and biological evolution. Nature 233:136.

71. Fonknechten N, Chaussonnerie S, Tricot S, Lajus A, Andreesen JR, Perchat N, Pelletier E, Gouyvenoux M, Barbe V, Salanoubat M. 2010. *Clostridium sticklandii*, a specialist in amino acid degradation: revisiting its metabolism through its genome sequence. BMC Genomics 11:555.

72. Pester M, Brambilla E, Alazard D, Rattei T, Weinmaier T, Han J, Lucas S, Lapidus A, Cheng J-F, Goodwin L. 2012. Complete genome sequences of *Desulfosporosinus orientis* DSM765T, *Desulfosporosinus youngiae* DSM17734T, Desulfosporosinus meridiei DSM13257T, and *Desulfosporosinus acidiphilus* DSM22704T. J Bacteriol194:6300-6301.

73. Hausmann B, Pelikan C, Rattei T, Loy A, Pester M. 2019. Long-term transcriptional activity at zero growth of a cosmopolitan rare biosphere member. mBio 10:e02189-18.

74. de Bok FA, Stams AJ, Dijkema C, Boone DR. 2001. Pathway of propionate oxidation by a syntrophic culture of *Smithella propionica* and *Methanospirillum hungatei*. Appl Environ Microbiol 67:1800-1804.

75. Sieber JR, Sims DR, Han C, Kim E, Lykidis A, Lapidus AL, McDonnald E, Rohlin L, Culley DE, Gunsalus R. 2010. The genome of *Syntrophomonas wolfei*: new insights into syntrophic metabolism and biohydrogen production. Environ Microbiol 12:2289-2301.

76. Yamamoto K, Tamaki H, Cadillo-Quiroz H, Imachi H, Kyrpides N, Woyke T, Goodwin L, Zinder SH, Kamagata Y, Liu W-T. 2014. Complete genome sequence of *Methanoregula formicica* SMSPT, a mesophilic hydrogenotrophic methanogen isolated



Applied and Environmental Microbiology
AEM
Applied and Environmental Microbiology

Accepted Manuscript Posted Online

from a methanogenic upflow anaerobic sludge blanket reactor. Genome Announc 2:e00870-14.

77. Bräuer S, Cadillo-Quiroz H, Kyrpides N, Woyke T, Goodwin L, Detter C, Podell S, Yavitt JB, Zinder SH. 2015. Genome of *Methanoregula boonei* 6A8 reveals adaptations to oligotrophic peatland environments. Microbiology 161:1572-1581.

78. Kraev G, Rivkina E, Vishnivetskaya T, Belonosov A, van Huissteden J, Kholodov A, Smirnov A, Kudryavtsev A, Teshebaeva K, Zamolodchikov D. 2019. Methane in gas shows from boreholes in epigenetic permafrost of Siberian Arctic. Geosciences, 9:67.

79. Lennon J, Muscarella M, Placella S, Lehmkuhl B. 2018. How, When, and Where Relic DNA Affects Microbial Diversity. mBio 9:e00637-18.

80. Starnawski P, Bataillon T, Ettema TJ, Jochum LM, Schreiber L, Chen X, Lever MA, Polz MF, Jørgensen BB, Schramm A. 2017. Microbial community assembly and evolution in subseafloor sediment. Proc Natl Acad Sci 114:2940-2945.

Applied and Environmental Microbiology

AEM

Applied and Environmental Microbiology

Accepted Manuscript Posted Online

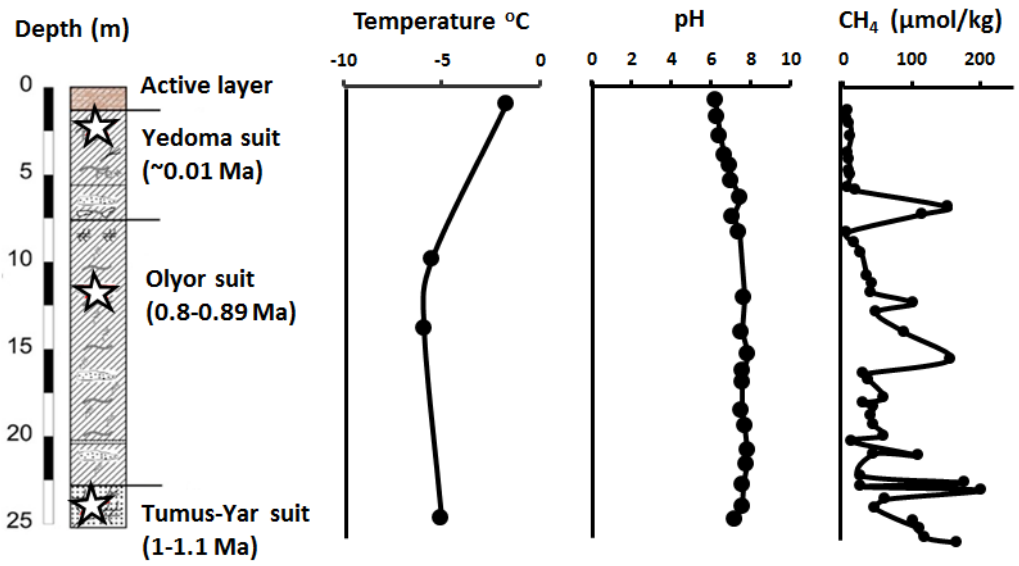


FIG. 1. Diagram of core sediment (0.0-25.05 m) from borehole AL1-15. The temperature, pH and concentration of $CH_4$ at various depths are shown on the right of the diagram. The stars indicate the depth of samples (1.4, 11.8 and 24.8 m) that were selected for Asp racemization and DNA extraction for microbial community characterization.



Applied and Environmental Microbiology
AEM
Applied and Environmental Microbiology

Accepted Manuscript Posted Online

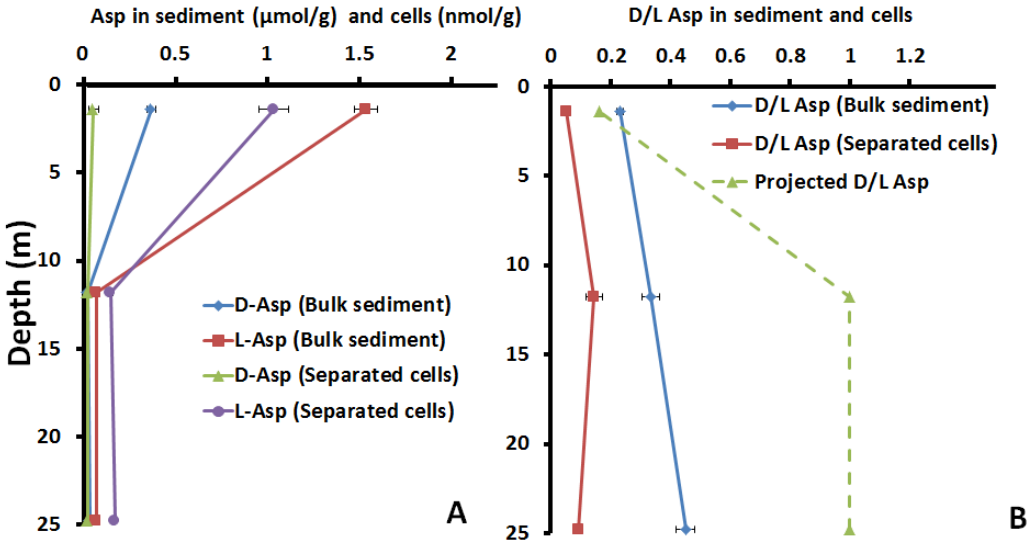


804

805

806 FIG. 2. (A) D and L-Aspartic acid concentration in bulk sediment and separated cells. (B) D/L

807 Asp in bulk sediment and separated cells and projected D/L Asp according to Asp racemization

808 model using the geological age of permafrost.



Applied and Environmental Microbiology
AEM
Applied and Environmental Microbiology

Accepted Manuscript Posted Online

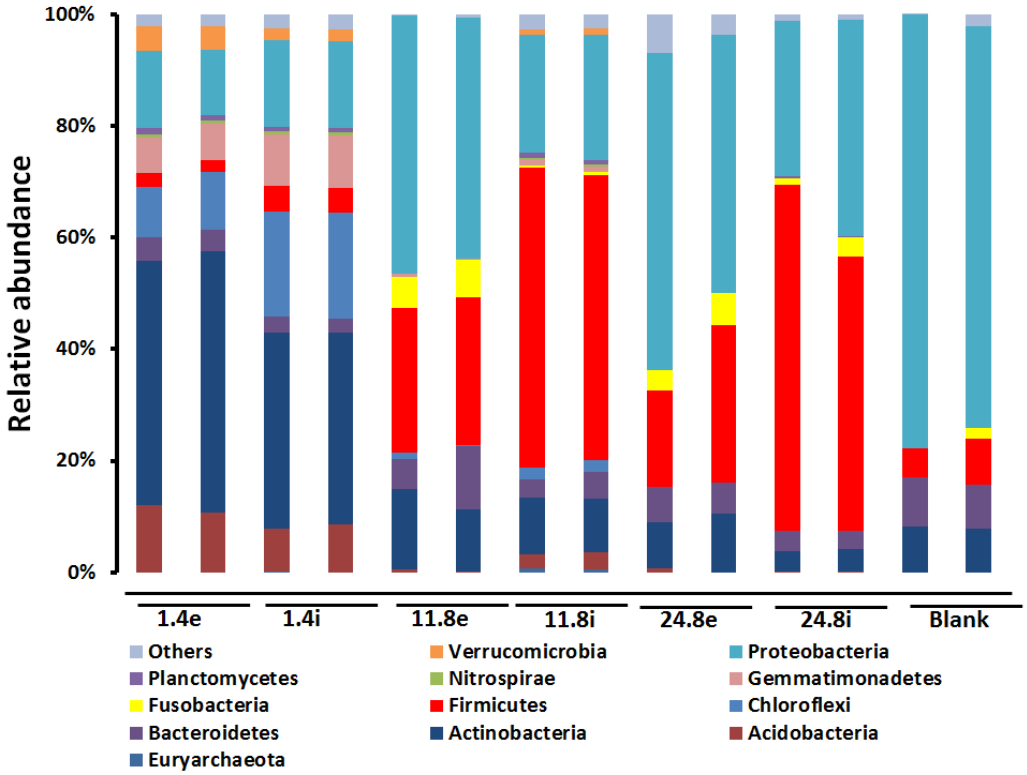


FIG. 3. Comparison of microbial community composition at phylum level determined by 16S rRNA amplicon sequencing. Only major phyla represent >1% the whole microbial community are shown for bacteria.



Applied and Environmental Microbiology
AEM
Applied and Environmental Microbiology

Accepted Manuscript Posted Online

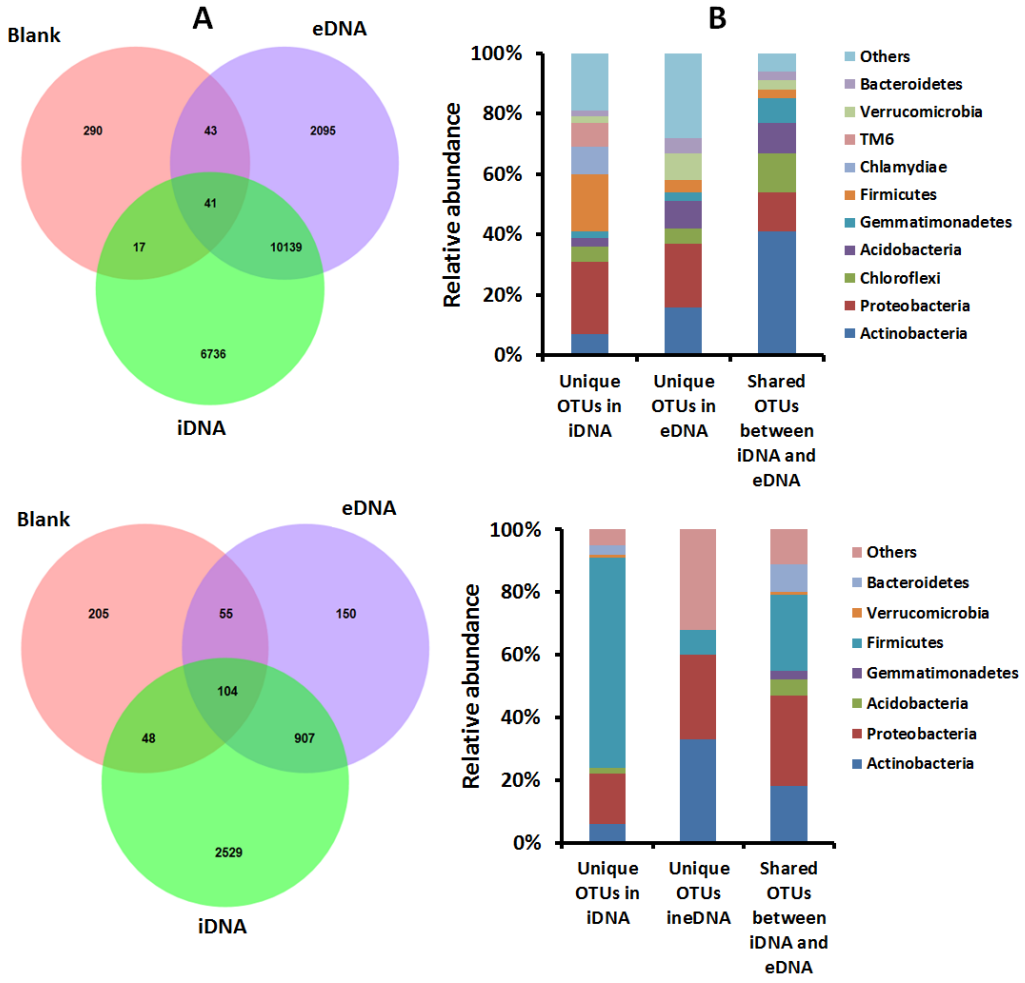


FIG. 4. (A) Venn diagrams of OTUs from eDNA, iDNA and extraction blanks, and (B) taxonomic distributions iDNA, eDNA and shared OTUs from sediments at 1.4 m (top) and 11.8 m (bottom).



Applied and Environmental Microbiology
AEM
Applied and Environmental Microbiology

Accepted Manuscript Posted Online

Applied and Environmental Microbiology

AEM

Applied and Environmental Microbiology

824

825

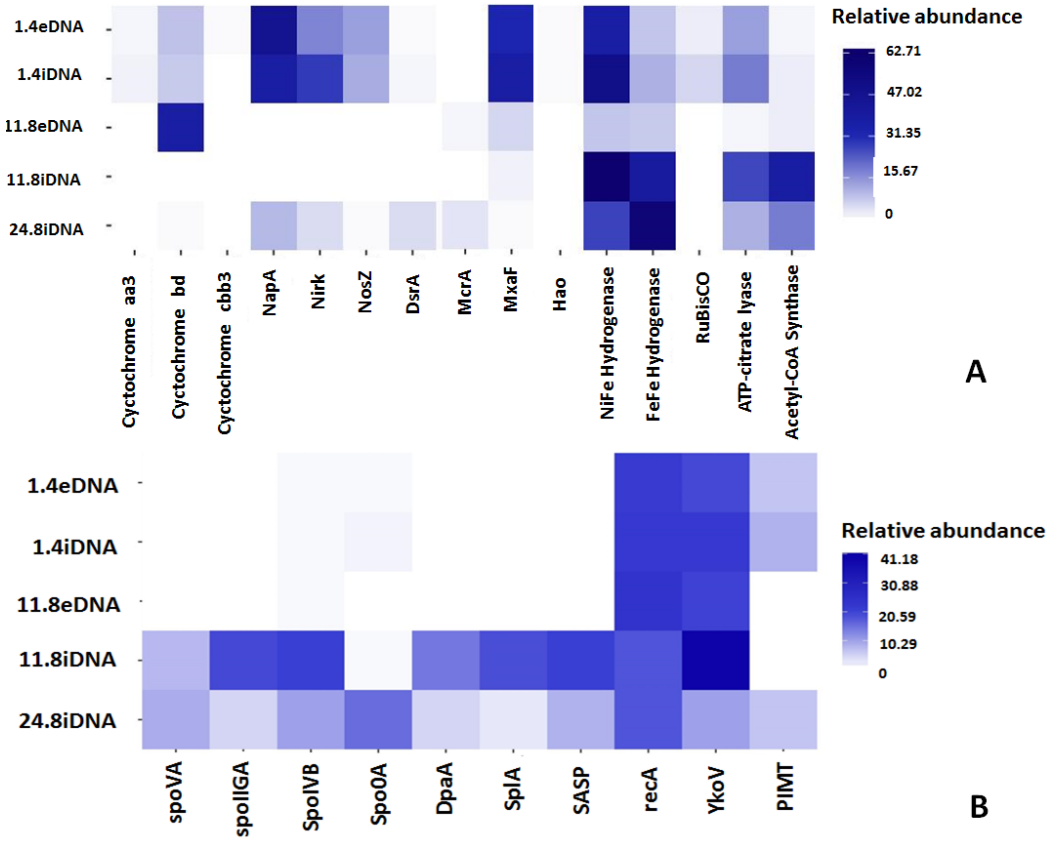


826

827

828 FIG. 5. (A) Relative abundance of functional genes related metabolisms with different electron

829 acceptors. (B) Long-term survival mechanisms including sporulation and DNA repair associated

830 genes.

831

Accepted Manuscript Posted Online

Applied and Environmental Microbiology

AEM

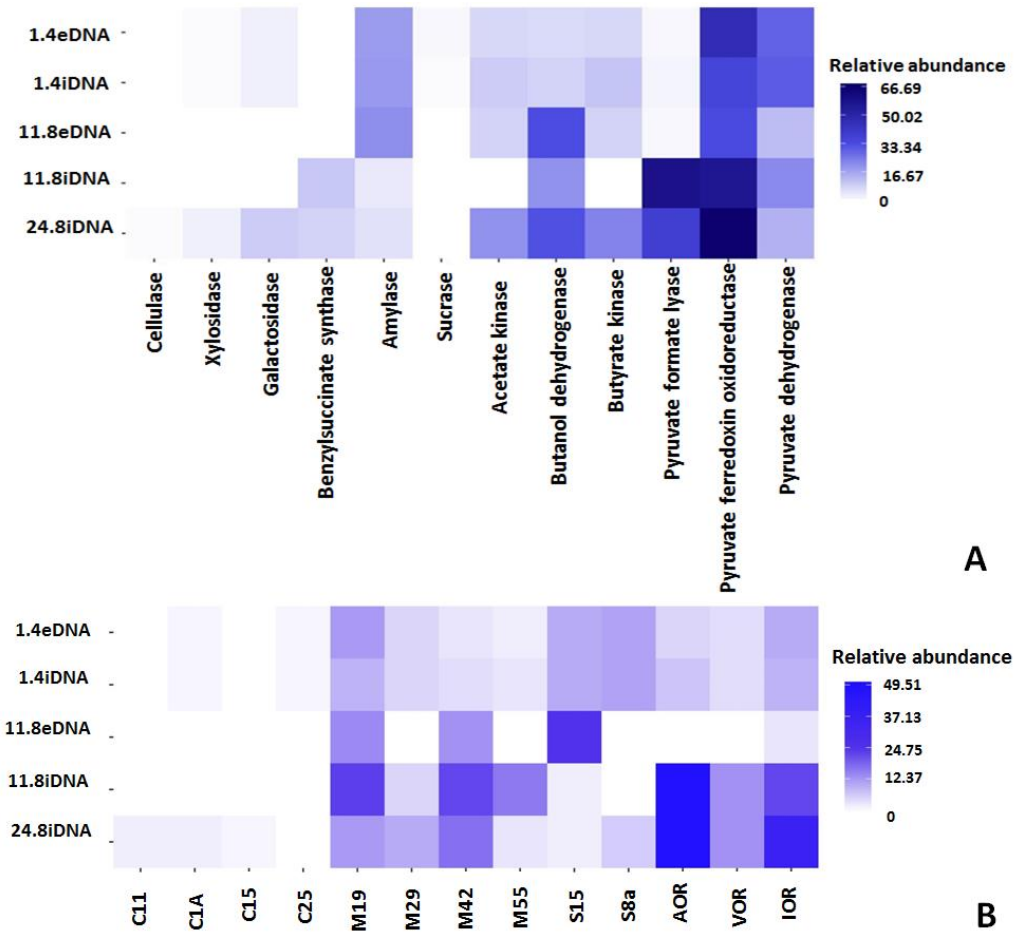


FIG. 6. Relative abundance of functional genes related to (A) carbohydrates and (B) fermentation of peptides and amino acids.

Accepted Manuscript Posted Online
Applied and Environmental Microbiology
AEM
Applied and Environmental Microbiology

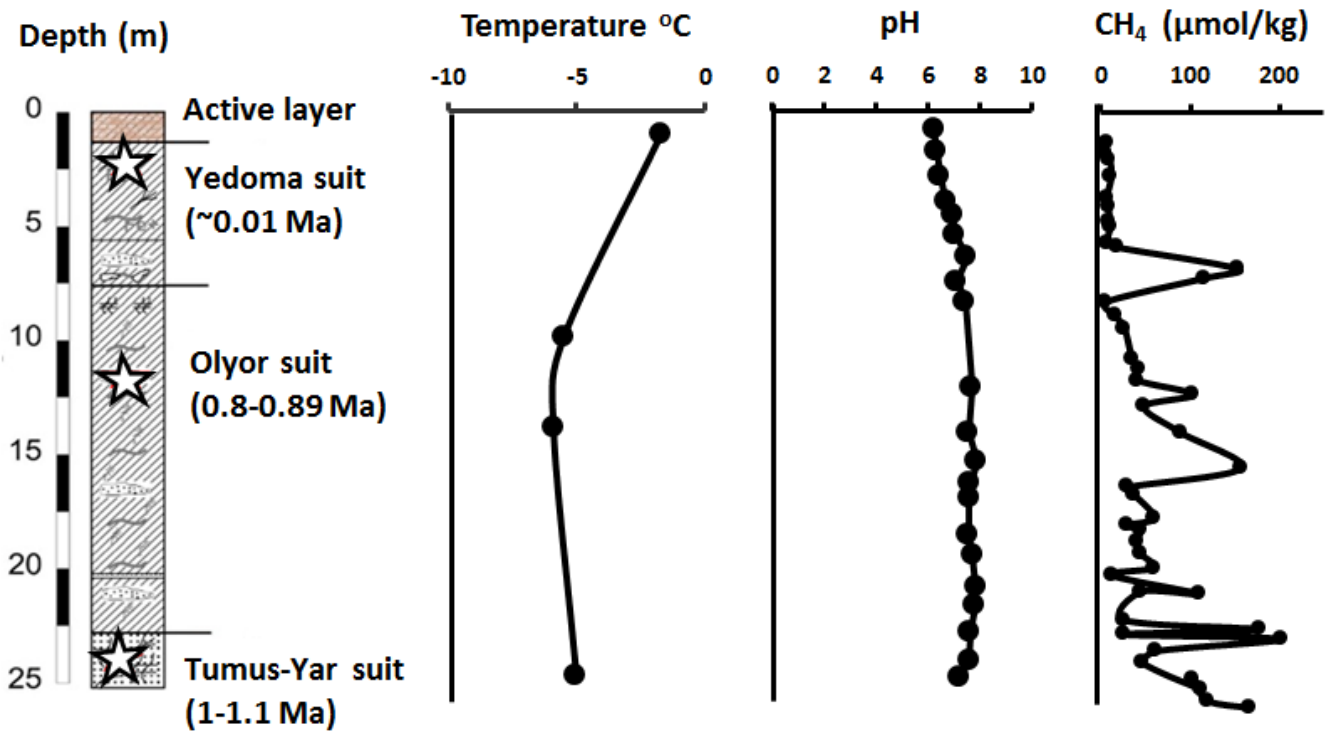

Accepted Manuscript Posted Online
Applied and Environmental Microbiology
AEM
Applied and Environmental Microbiology

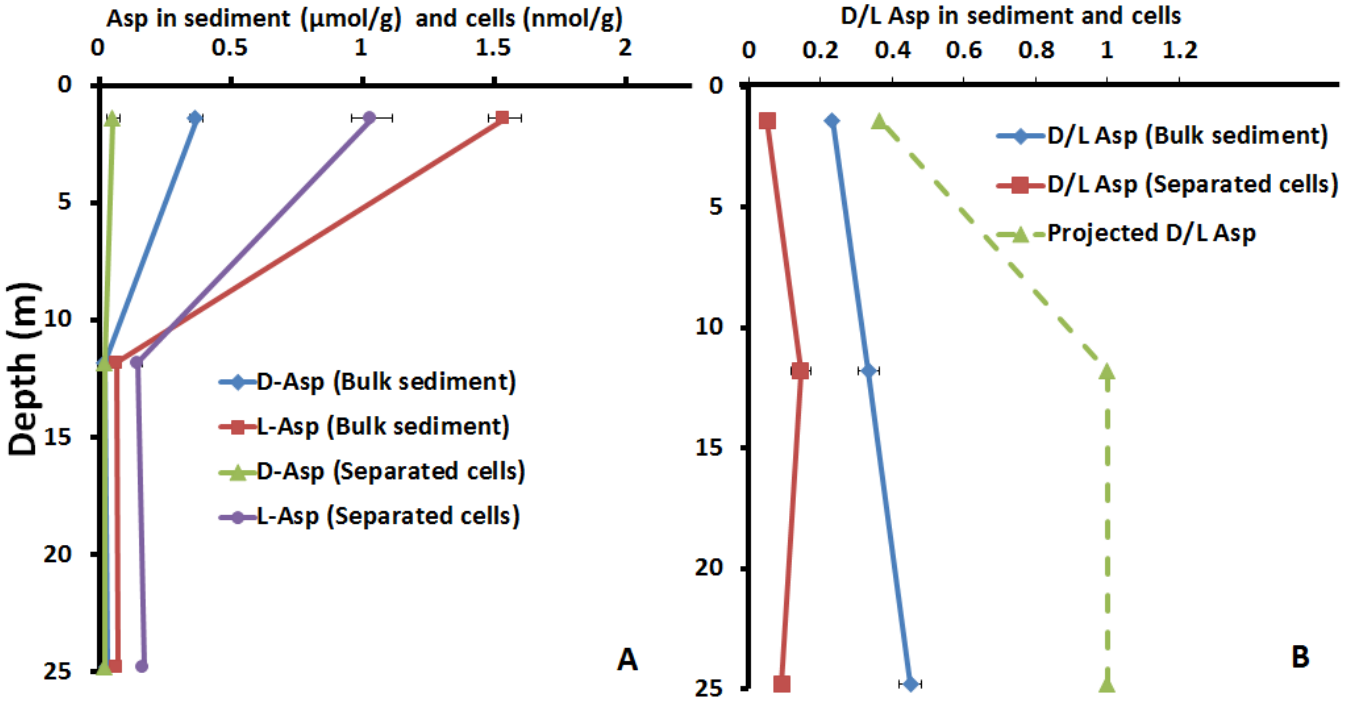

Accepted Manuscript Posted Online
Applied and Environmental Microbiology
AEM
Applied and Environmental Microbiology

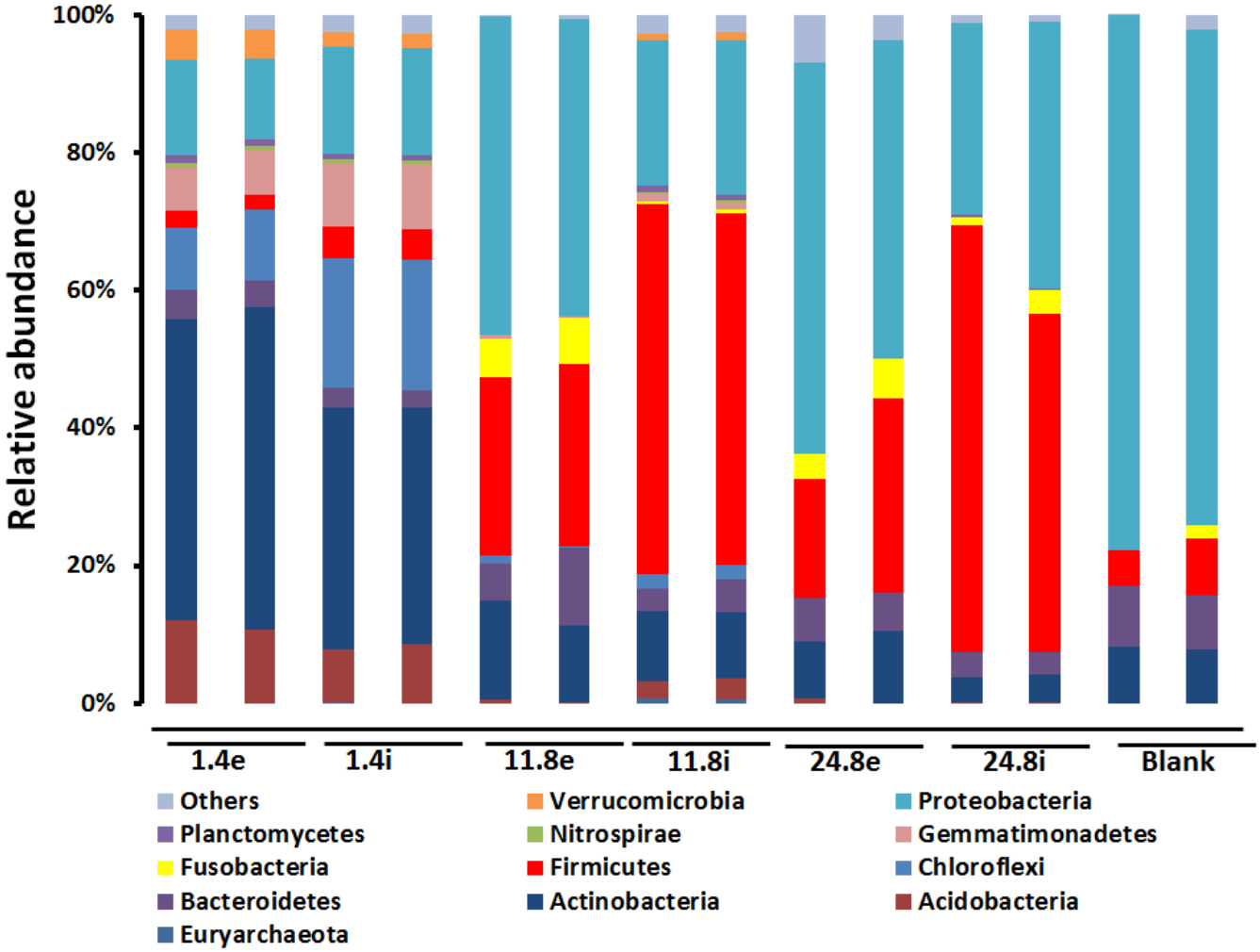

Accepted Manuscript Posted Online
Applied and Environmental Microbiology
AEM
Applied and Environmental Microbiology

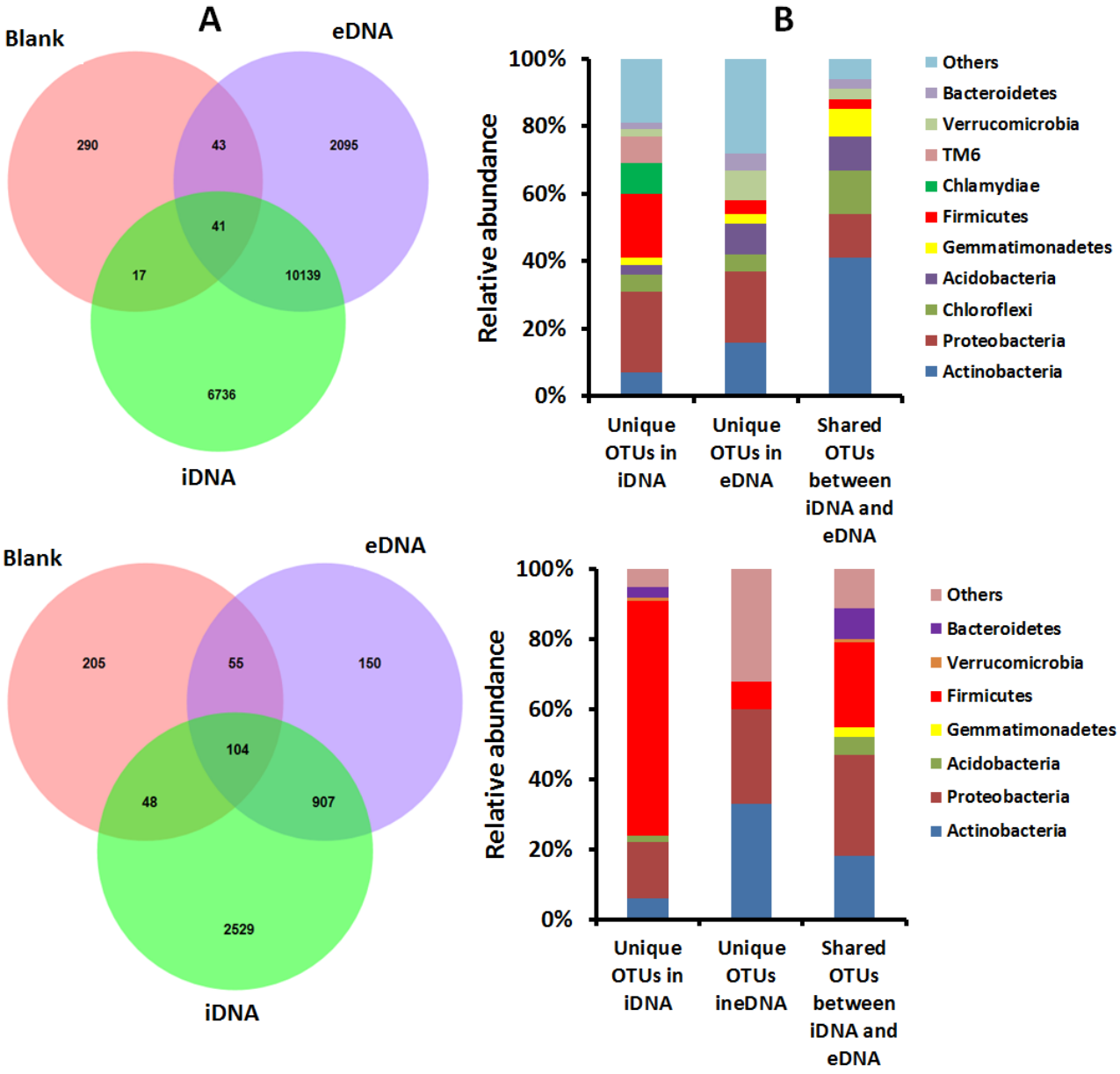

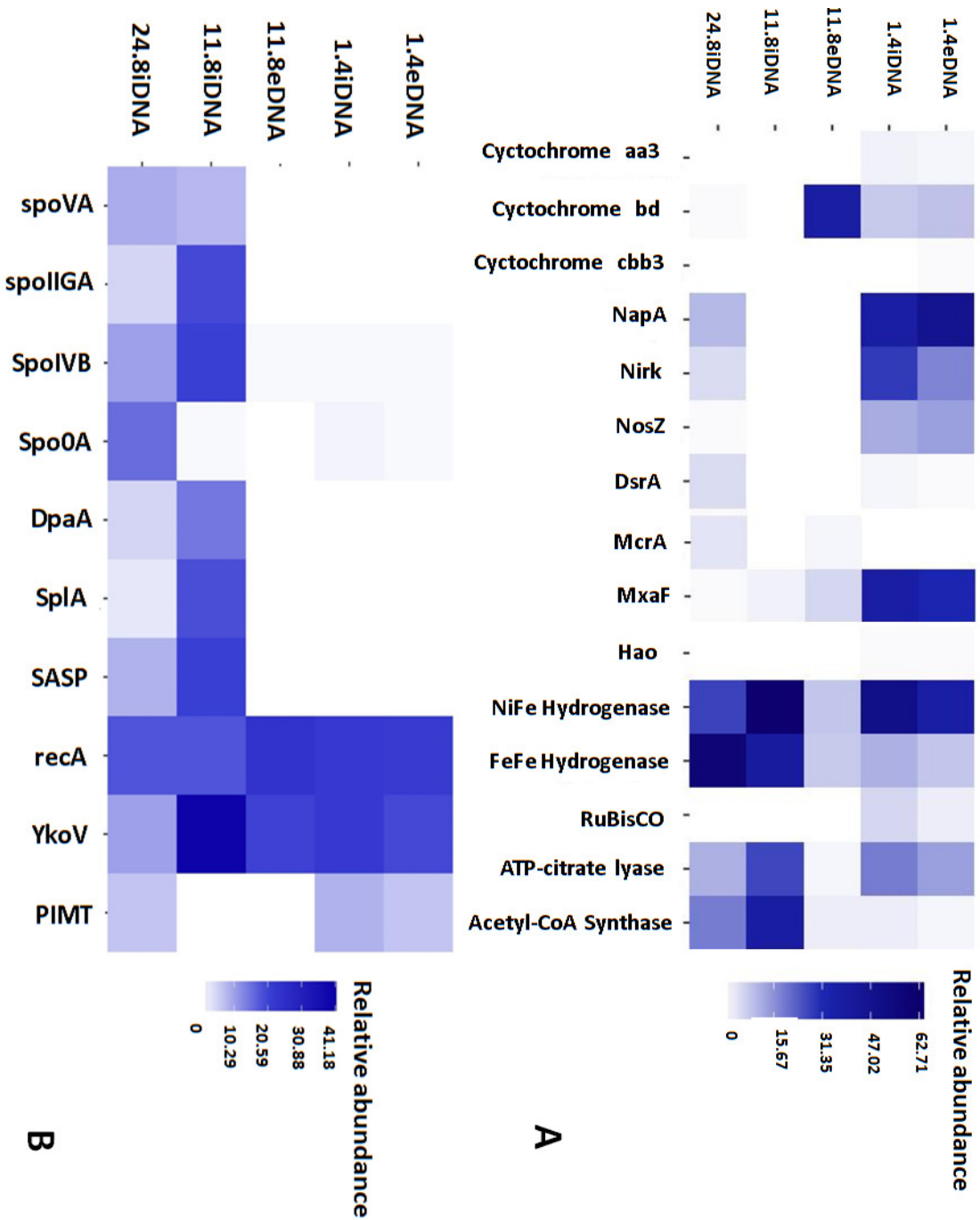
24.8iDNA
11.8iDNA
11.8eDNA
1.4iDNA
1.4eDNA
spoVA
spoIIGA
SpoIVB
Spo0A
DpaA
SplA
SASP
recA
YkoV
PIMT
0
10.29
20.59
30.88
41.18
Relative abundance
B
Cyctochrome aa3
Cyctochrome bd
Cyctochrome cbb3
NapA
Nirk
NosZ
DsrA
McrA
MxaF
Hao
NiFe Hydrogenase
FeFe Hydrogenase
RuBisCO
ATP-citrate lyase
Acetyl-CoA Synthase
0
15.67
31.35
47.02
62.71
Relative abundance
A

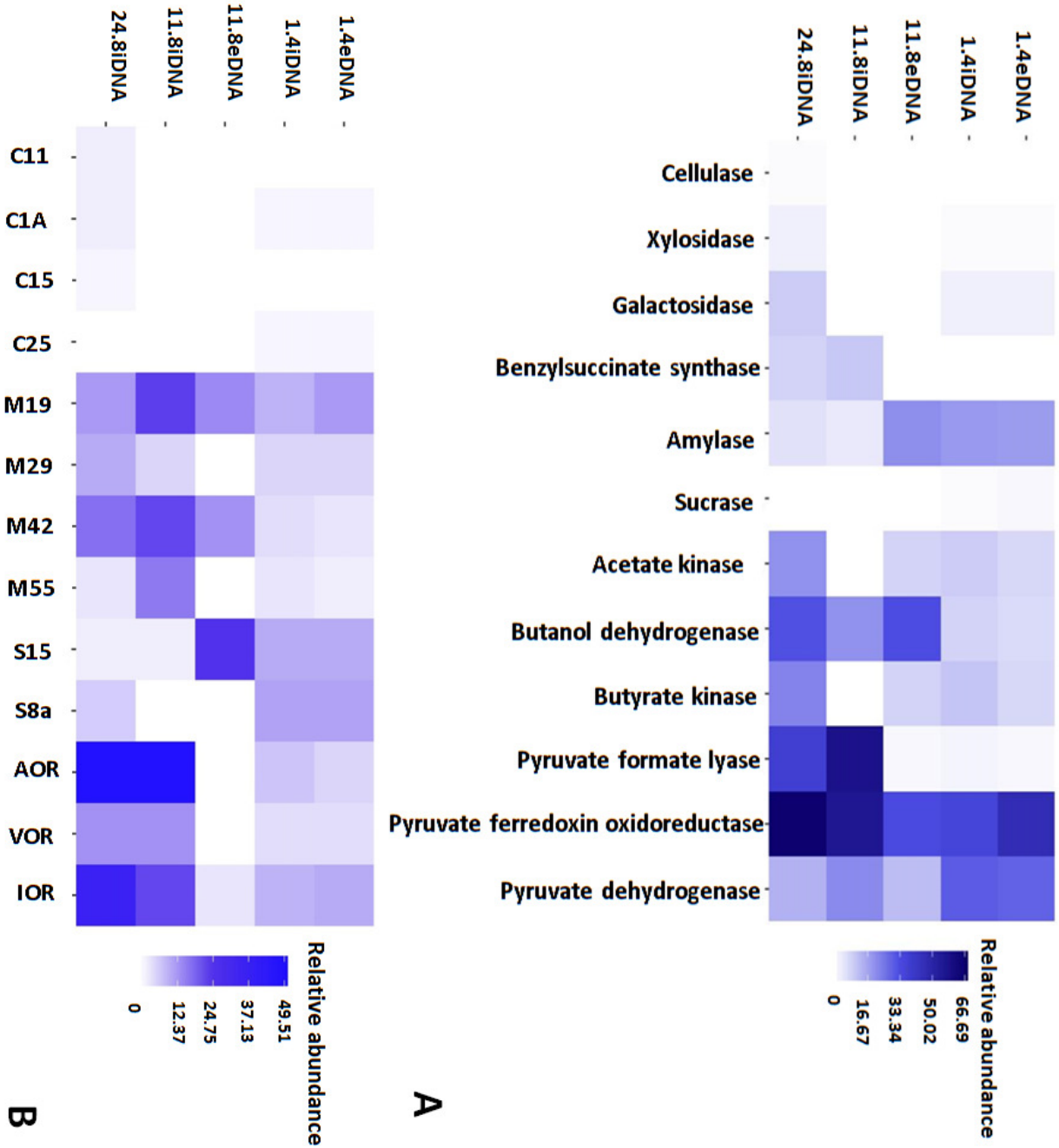
24.8iDNA
11.8iDNA
11.8eDNA
1.4iDNA
1.4eDNA
Cellulase
Xylosidase
Galactosidase
Benzylsuccinate synthase
Amylase
Sucrase
Acetate kinase
Butanol dehydrogenase
Butyrate kinase
Pyruvate formate lyase
Pyruvate ferredoxin oxidoreductase
Pyruvate dehydrogenase
0
16.67
33.34
50.02
66.69
Relative abundance
A
C11
C1A
C15
C25
M19
M29
M42
M55
S15
S8a
AOR
VOR
IOR
0
12.37
24.75
37.13
49.51
Relative abundance
B